



---

## Figures and figure supplements

A composition-dependent molecular clutch between T cell signaling condensates and actin

**Jonathon A Ditlev et al**

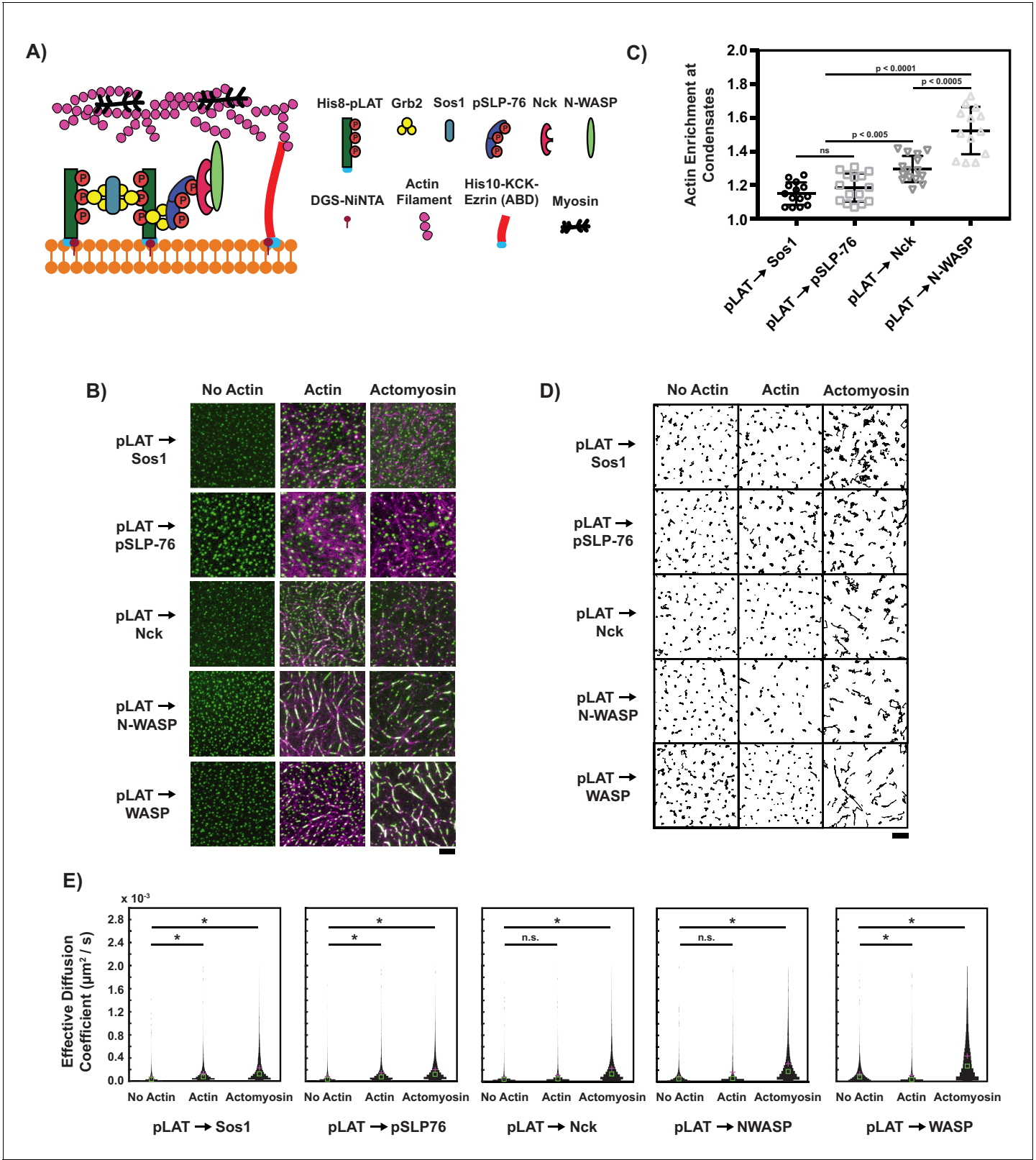


*Figure 1 continued*

actomyosin networks (right column). pLAT-Alexa488 is green, rhodamine-actin is magenta. Scale bar = 5  $\mu\text{m}$ . (C) Actin enrichment at condensates in reconstitution assays using actomyosin, calculated as the ratio of actin fluorescence intensity within condensates to actin intensity outside condensates (see Materials and methods). Shown are the individual data points and their mean  $\pm$ s.d. from N = 15 fields of view from three independent experiments (with 5 FOV per experiment). P-values are for indicated distribution comparisons via Wilcoxon rank-sum test with Bonferroni correction to achieve a total type-I error of 0.05. (D) Example plots of condensate tracks. Scale bar = 5  $\mu\text{m}$ . (E) Effective diffusion coefficients of the condensate tracks. Each measurement is shown as a violin plot of the distribution of values from analyzing N = 15 fields of view from three independent experiments (with 5 FOV per experiment). Green square shows median and magenta plus sign shows mean. Significance was determined by averaging results from 100 Wilcoxon rank-sum tests that compared pairs of 500 randomly-selected tracks.

DOI: <https://doi.org/10.7554/eLife.42695.002>

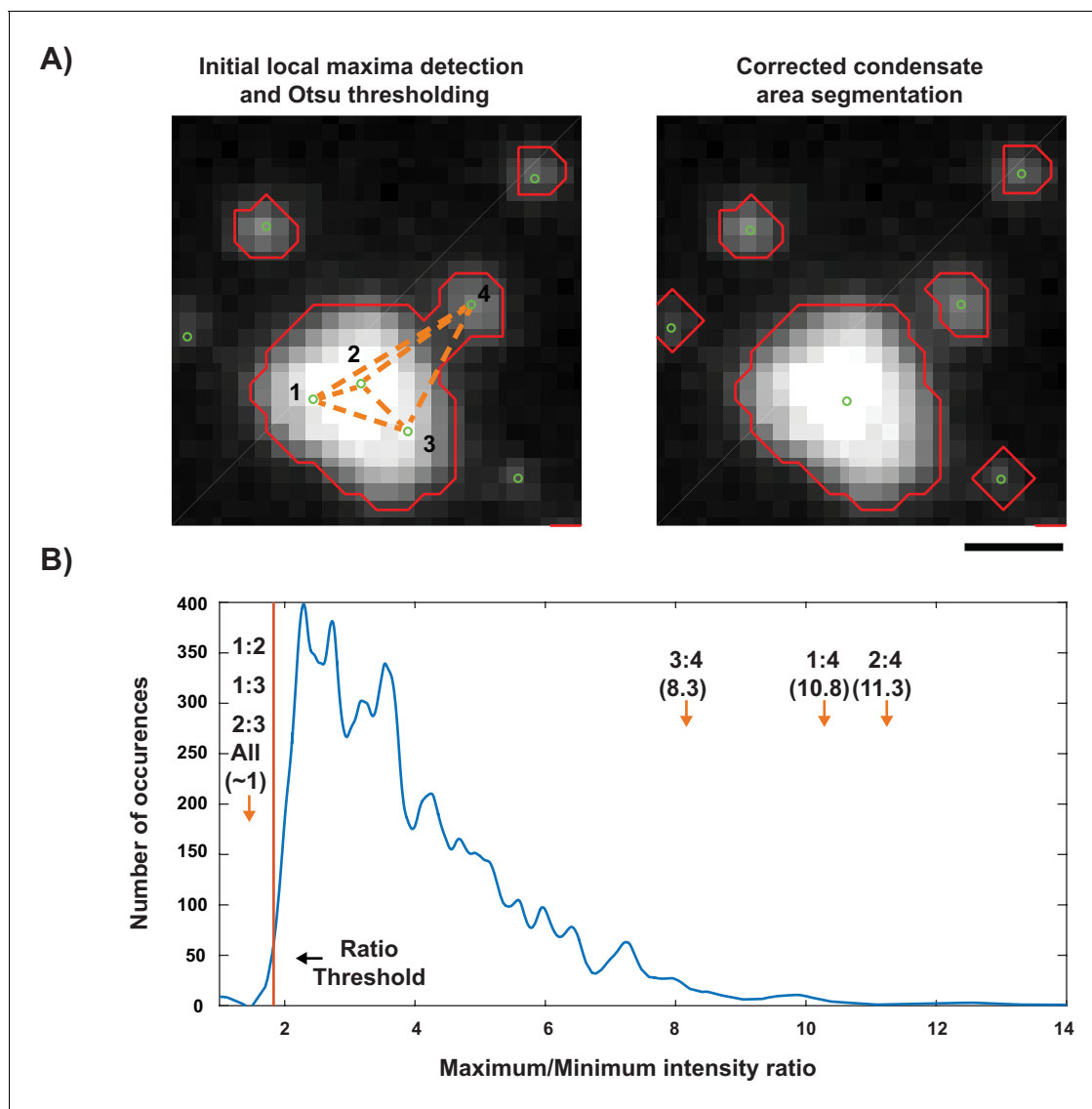


**Figure 1—figure supplement 1.** Detection process for LAT condensates in vitro. (A) (left) An example of the initial thresholding and local maxima detection for LAT condensates. Orange dotted lines indicate pair-wise comparisons that are made to remove superfluous local maxima. (right) Thresholded areas and local maxima after correction steps. (B) The distribution of maximum/minimum intensity ratios taken from segmented areas with a single local maximum. The threshold (1<sup>st</sup> percentile of distribution) used to discard local maxima is shown as an orange line. The maximum/minimum intensity ratios of the pairs from (A) are shown with orange arrows.

DOI: <https://doi.org/10.7554/eLife.42695.003>



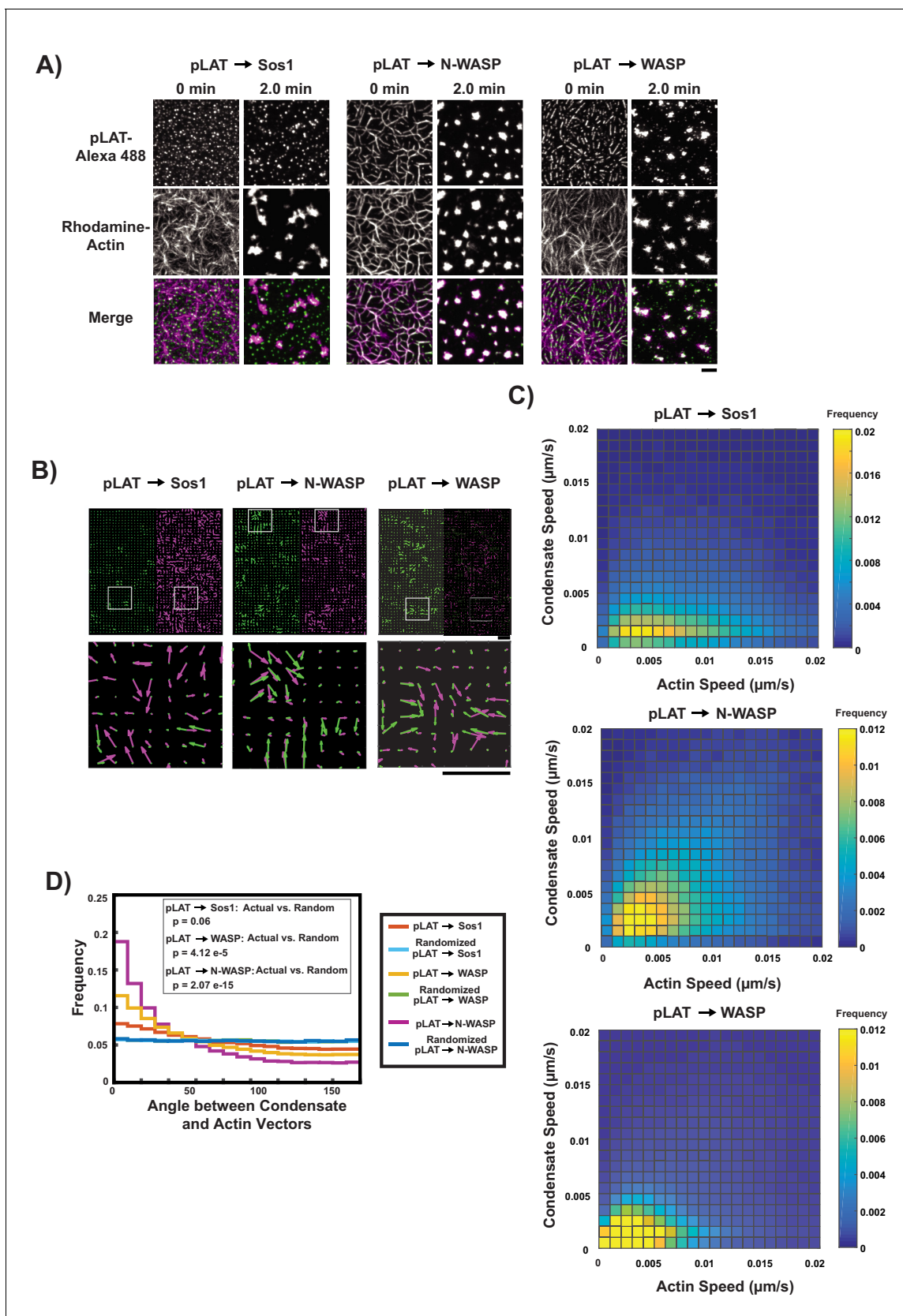


**Figure 2.** pLAT → N-WASP condensates bind to and move with moving actin filaments. (A) TIRF microscopy images of pLAT → Sos1 condensates (left two columns), and pLAT → N-WASP condensates (middle two columns), and pLAT → WASP (right two columns), formed in an actin network before Figure 2 continued on next page

*Figure 2 continued*

( $t = 0$  min) and after ( $t = 2$  min) addition of myosin II. pLAT condensates are green and actin is magenta in merge. Scale bar =  $5\ \mu\text{m}$ . (B–D) STICS analysis of actin and condensate movement. (B) Representative map of actin (magenta) and pLAT condensate (green) vector fields. Lower panels show magnification of box regions in upper panels. (C) Condensate speed vs. actin speed at same position. Condensate composition indicated above each heat map. Heat map indicates frequency in each bin, that is counts in each bin normalized by total number of counts. (D) Distribution of the angle between actin and condensate movement vectors for pLAT  $\rightarrow$  Sos1 (blue), pLAT  $\rightarrow$  N-WASP (gold), randomized pLAT  $\rightarrow$  Sos1 (red) and randomized pLAT  $\rightarrow$  N-WASP (purple) (see Materials and methods for randomization). P-values are for indicated distribution comparisons via Kolmogorov-Smirnov test. Data in (C) and (D) are pooled from 15 fields of view from three independent experiments (5 FOV per experiment).

DOI: <https://doi.org/10.7554/eLife.42695.008>

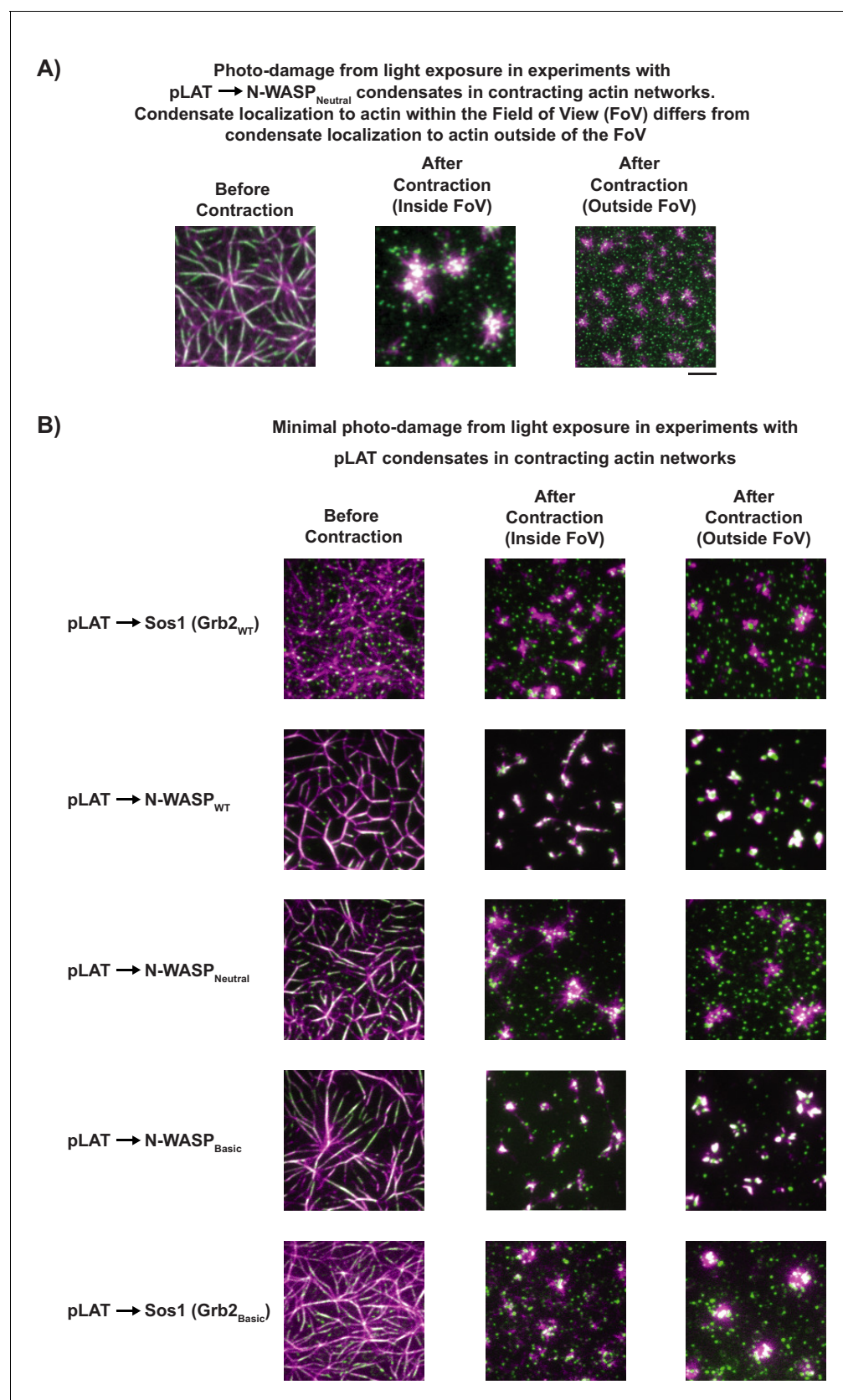


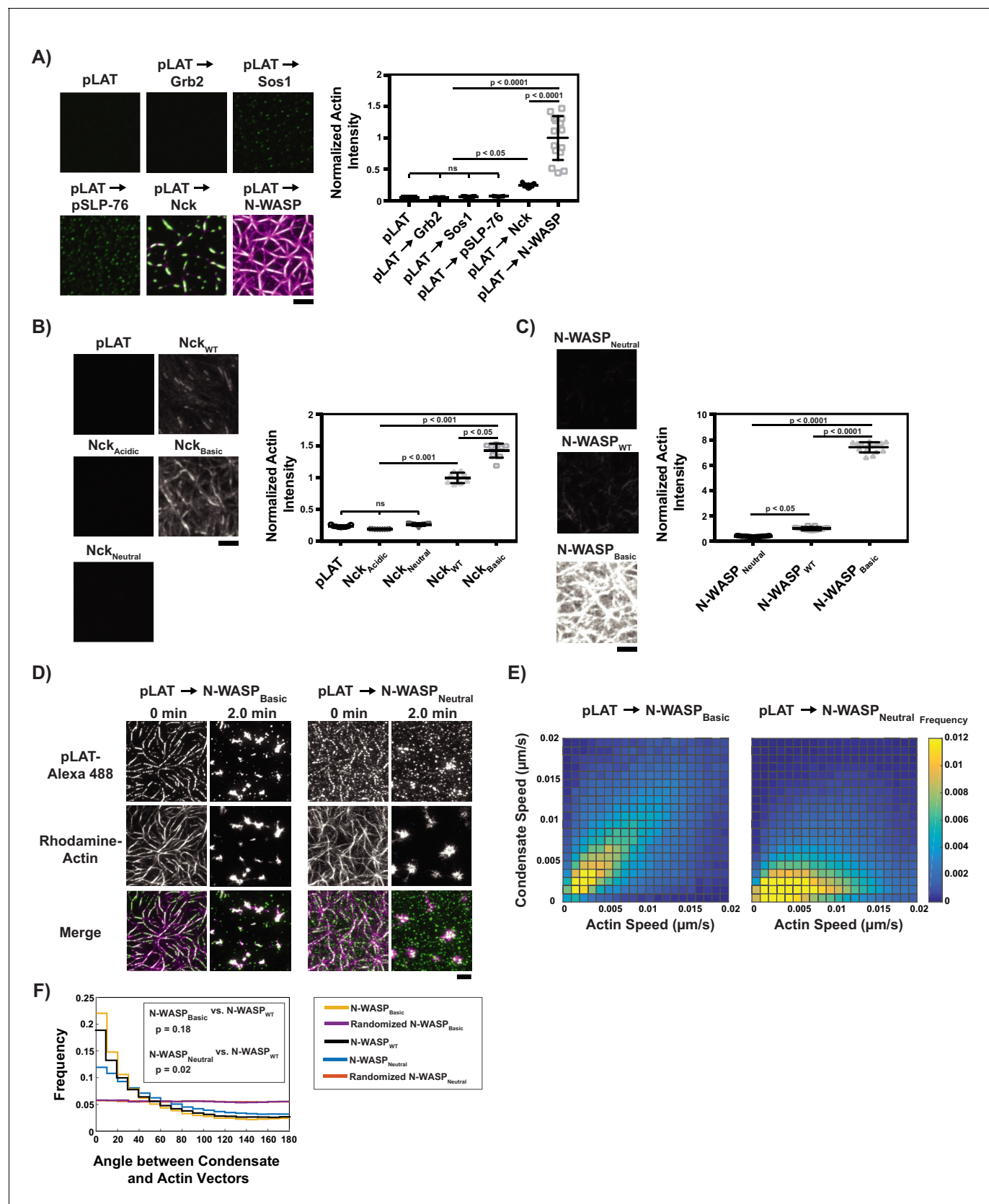
**Figure 2—figure supplement 1.** In actomyosin contractile assays, imaging conditions were chosen such that photo-damage was minimized to avoid artifactual results. (A) TIRF microscopy images of LAT condensate movement following myosin II-induced actin contraction inside or outside the field of

*Figure 2—figure supplement 1 continued on next page*

*Figure 2—figure supplement 1 continued*

view (FOV) when care was not taken to minimize photo-damage. (left) Representative image of pLAT → N-WASP<sub>Neutral</sub> condensate (green) wetting of rhodamine-actin filaments (magenta) prior to induced actin contraction. (center) Image of same FOV after imaging during myosin II-induced actin contraction. (right) Image of region outside of FOV (i.e. not imaged during contraction) obtained immediately following actin contraction. Comparing center and right images indicates that photo-damage can increase interactions between condensates and actin, leading to artifactual co-localization following contraction. **(B)** When imaging is performed with low laser power (as done in our experiments), regions inside and outside of the FOV during actin contraction show similar co-localization of condensates with actin asters. Figure shows representative images for a variety of pLAT condensates types captured in the FOV prior to myosin II-induced actin contraction (left), in the FOV after myosin II-induced contraction (center), and outside of the FOV after contraction (right).

DOI: <https://doi.org/10.7554/eLife.42695.009>



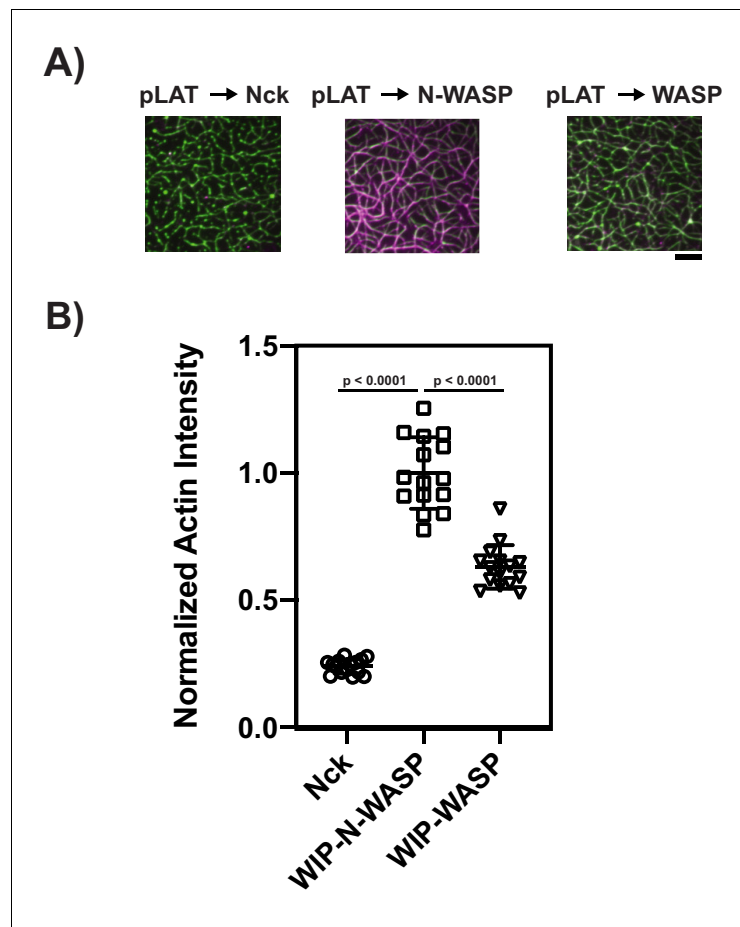
**Figure 3.** Basic regions of Nck and N-WASP mediate interaction of LAT condensates with actin filaments. (A) (Left) TIRF microscopy images of rhodamine-actin (magenta) recruited to SLBs by the indicated LAT condensate compositions (green). Scale bar = 5  $\mu$ m. All panels use the same

Figure 3 continued on next page

## Figure 3 continued

intensity range. (Right) Normalized average rhodamine-actin fluorescence intensity on SLBs. Shown are the individual data points and their mean  $\pm$ s.d. N = 15 fields of view from three independent experiments (5 FOV per experiment). P values were determined using a t-test. (B) (Left) TIRF microscopy images of rhodamine-actin recruited to SLBs by His-tagged Nck variants. Scale bar = 5  $\mu$ m. All panels use the same intensity range. (Right) Normalized average rhodamine-actin fluorescence intensity on SLBs. Shown are the individual data points and their mean  $\pm$ s.d. N = 9 fields of view from three independent experiments (3 FOV per experiment). P values were determined using a t-test. (C) (Left) TIRF microscopy images of rhodamine-actin recruited to SLBs by His-tagged N-WASP variants. All panels use the same intensity range. (Right) Normalized average rhodamine-actin fluorescence intensity on SLBs. Shown are the individual data points and their mean  $\pm$ s.d. N = 15 fields of view from three independent experiments (5 FOV per experiment). P values were determined using a t-test. (D) TIRF microscopy images of pLAT  $\rightarrow$  N-WASP<sub>Basic</sub> condensates (left two columns) and pLAT  $\rightarrow$  N-WASP<sub>Neutral</sub> condensates (right two columns) formed in an actin network before (t = 0 min) and after (t = 2 min) addition of myosin II. LAT condensates are green and actin is magenta in merge. Scale bar = 5  $\mu$ m. (E) Condensate speed vs. actin speed at same position from STICS analysis. Condensate composition indicated above each heat map. Heat map indicates frequency in each bin (as in **Figure 2C**). N = 15 fields of view from three independent experiments (5 FOV per experiments). (F) Distribution of the angle between actin and condensate movement vectors for pLAT  $\rightarrow$  N-WASP<sub>Basic</sub> (gold), randomized pLAT  $\rightarrow$  N-WASP<sub>Basic</sub> (purple), pLAT  $\rightarrow$  N-WASP<sub>WT</sub> (black, same data as in **Figure 2**), pLAT  $\rightarrow$  N-WASP<sub>Neutral</sub> (blue), and randomized pLAT  $\rightarrow$  N-WASP<sub>Neutral</sub> (red). N = 15 fields of view from three independent experiments (5 FOV per experiment). P-values are for indicated distribution comparisons via Kolmogorov-Smirnov test.

DOI: <https://doi.org/10.7554/eLife.42695.011>



**Figure 3—figure supplement 1.** pLAT → Nck, pLAT → N-WASP, and pLAT → WASP condensates bind F-Actin. (A) TIRF microscopy images of rhodamine-actin recruited to pLAT → Nck, pLAT → N-WASP, and pLAT → WASP condensates. Scale bar = 5  $\mu$ m. (B) Normalized average rhodamine-actin fluorescence intensity on SLBs. Shown are the individual data points and their mean  $\pm$ s.d. N = 15 fields of view from three independent experiments (5 FOV per experiment). P values were determined using a t-test.

DOI: <https://doi.org/10.7554/eLife.42695.012>



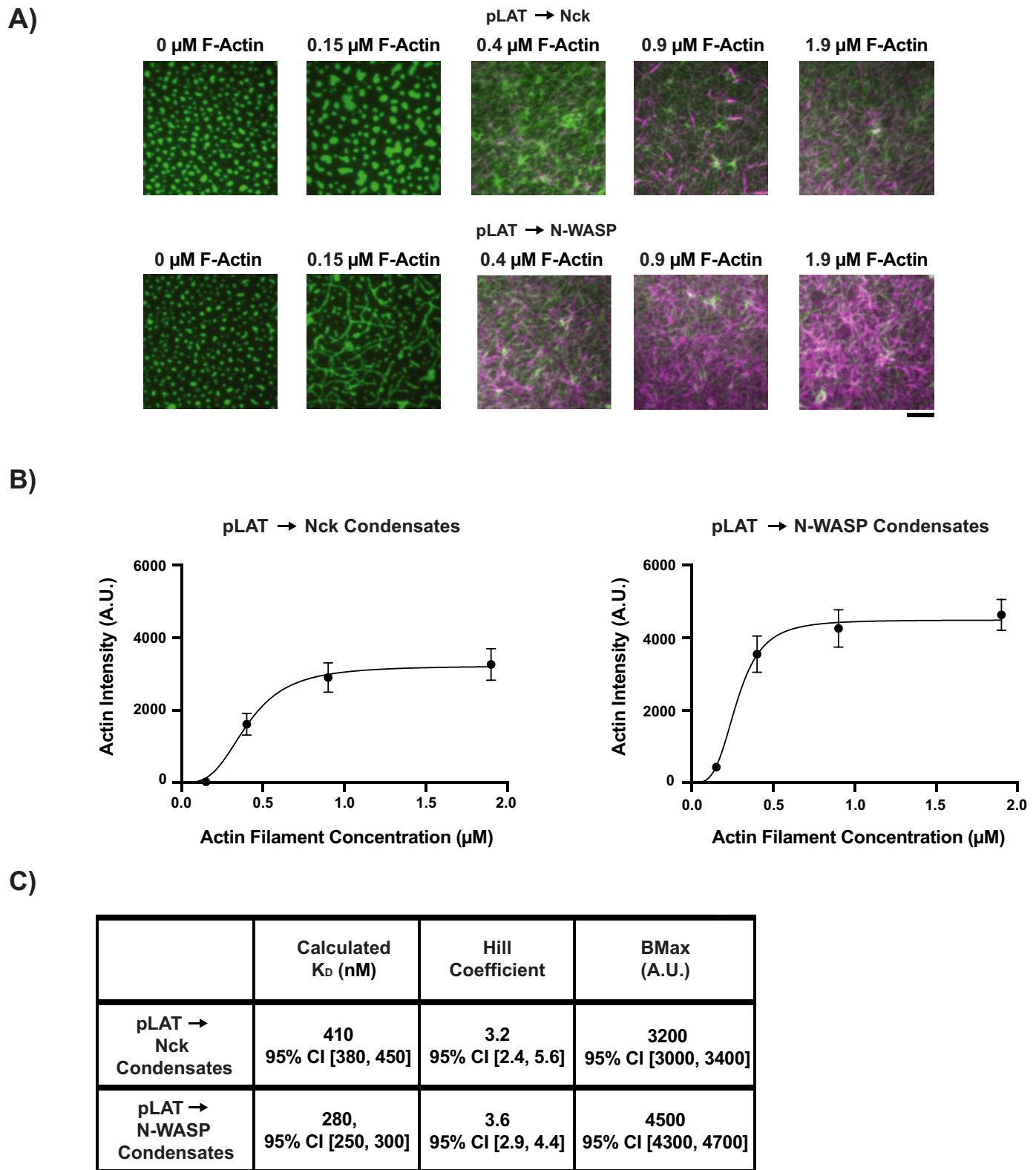


**Figure 3—figure supplement 2.** Quantitative analysis of actin filaments binding to LAT condensates. (A) TIRF microscopy images of rhodamine actin recruited to pLAT → Nck or pLAT → N-WASP condensates. Scale bar = 5  $\mu$ m. (B) Plots of fluorescence intensity of rhodamine actin recruited to the

Figure 3—figure supplement 2 continued on next page



*Figure 3—figure supplement 2 continued*

SLB. Shown are the average intensity value for each concentration of rhodamine actin  $\pm$ s.d. from  $N = 15$  fields of view from three independent experiments (5 FOV per experiment). Data was fit using the Specific Binding with a Hill slope algorithm in GraphPad Prism. (C) Calculated  $K_D$ , Hill Coefficient, and binding capacity ( $B_{Max}$ ) for pLAT  $\rightarrow$  Nck and pLAT  $\rightarrow$  N-WASP condensates using the fit shown in (B).

DOI: <https://doi.org/10.7554/eLife.42695.014>

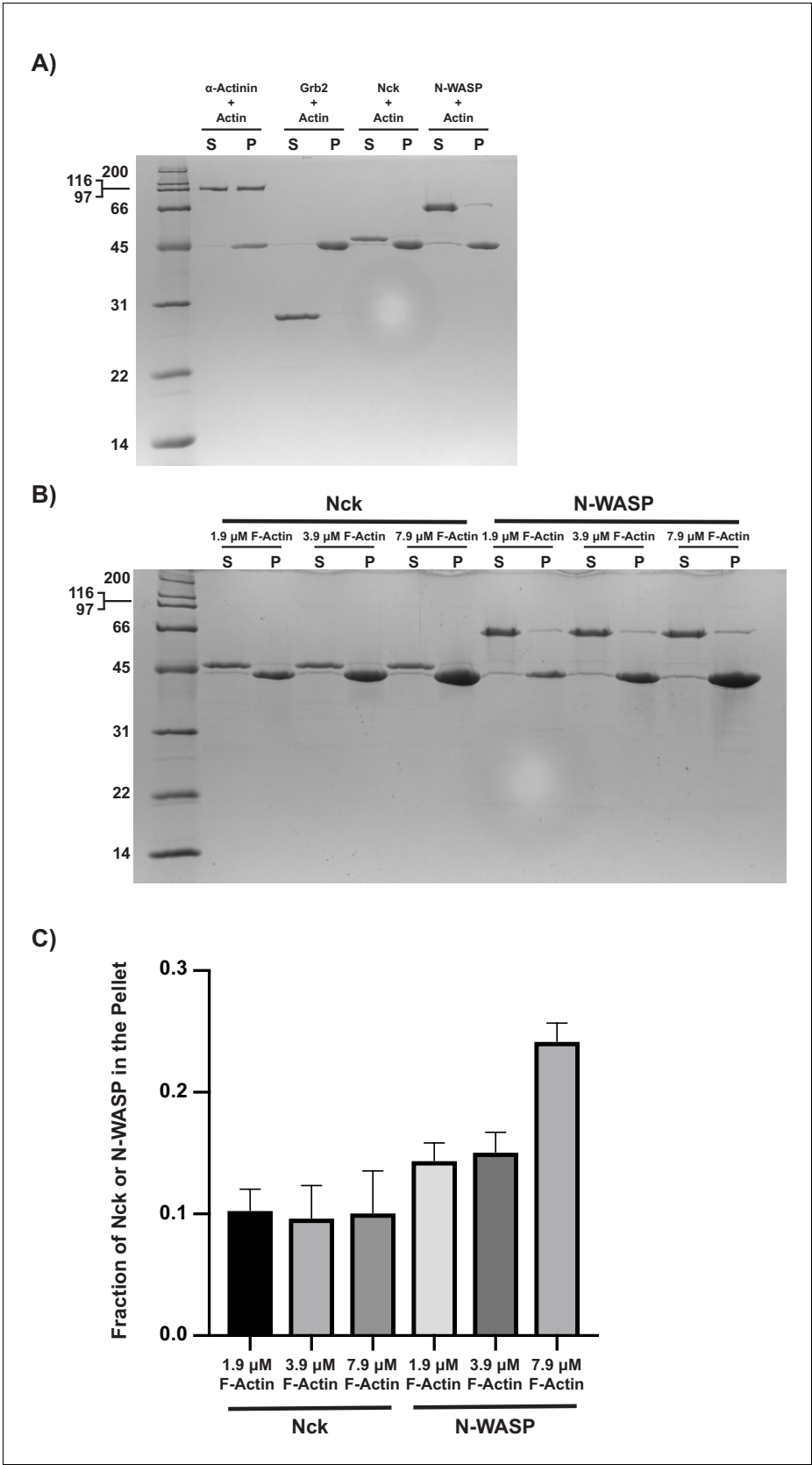


**Figure 3—figure supplement 3.** Nck does not co-sediment with actin filaments. N-WASP co-sediments with actin filaments, but not to the same degree as  $\alpha$ -actinin, a known actin filament binding protein. **(A)** Coomassie blue-  
Figure 3—figure supplement 3 continued on next page

*Figure 3—figure supplement 3 continued*

stained SDS-PAGE gel showing co-sedimentation of  $\alpha$ -actinin (positive control), Grb2 (negative control), Nck, and N-WASP with actin filaments. **(B)** Coomassie blue-stained SDS-PAGE gel showing co-sedimentation of Nck or N-WASP with increasing actin filament concentration. **(C)** Quantification of Nck and N-WASP bands shown in **(B)**. Error bars report  $\pm$ s.d. from N = 3 independent co-sedimentation assays and gels.

DOI: <https://doi.org/10.7554/eLife.42695.017>

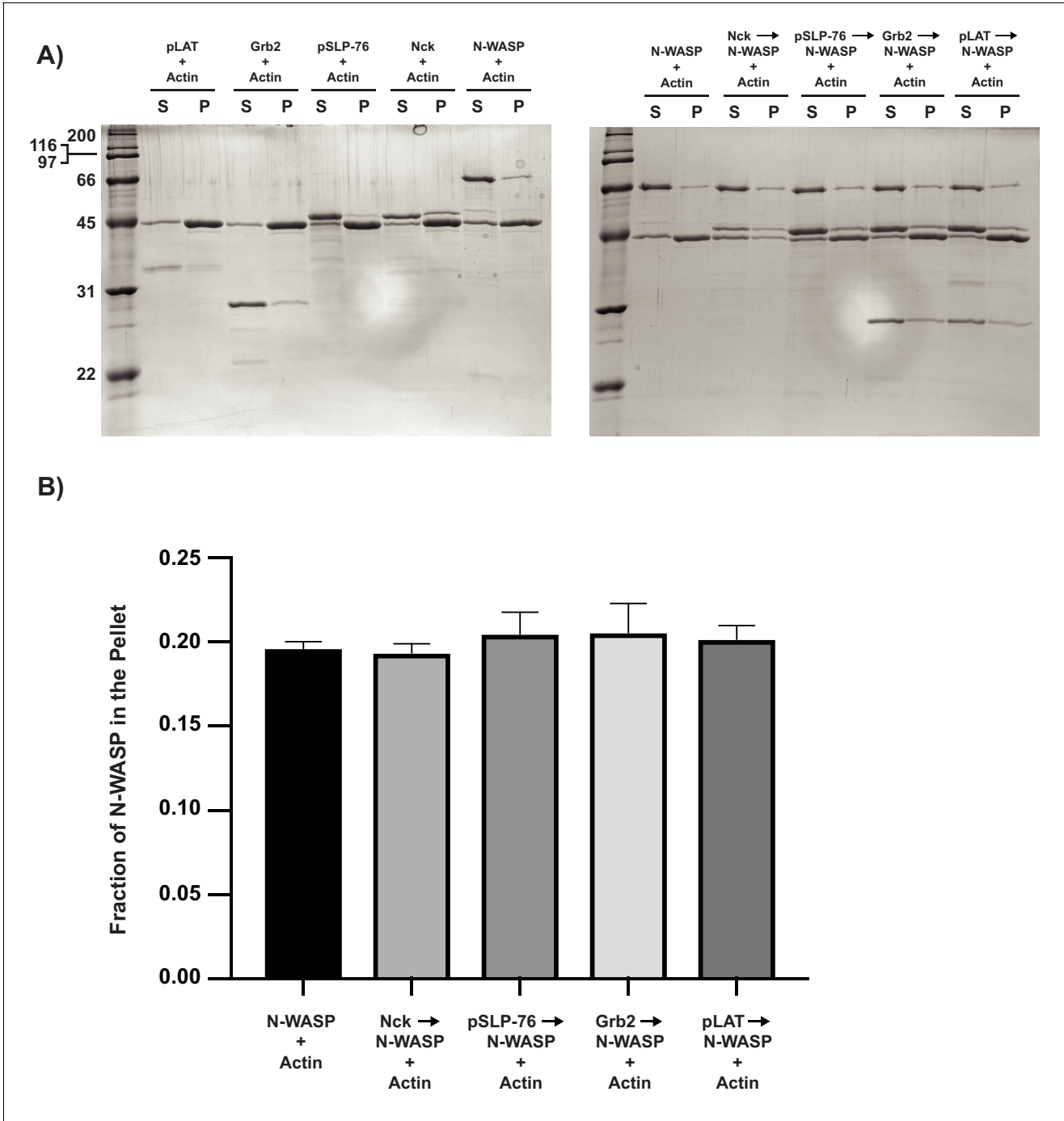


**Figure 3—figure supplement 4.** N-WASP binding partners do not increase N-WASP co-sedimentation with F-actin. (A) (Left) Coomassie blue-stained SDS-PAGE gel showing co-sedimentation of pLAT, Grb2, pSLP-76, Nck, and N-WASP with actin filaments. (Right) Coomassie blue-stained SDS-PAGE gel showing co-sedimentation of N-WASP, Nck + N-WASP, pSLP-76 + Nck + N-WASP, Grb2 + pSLP-76 + Nck + N-WASP, and pLAT + Grb2 + pSLP-76 + Nck + N-WASP with actin filaments. It should be noted that pLAT is weakly stained by Coomassie blue, and thus the band appears fainter than other bands. (B) Quantification of N-WASP bands shown in (A). Error bars report  $\pm$ s.d. from N = 3 independent co-sedimentation assays and gels.

DOI: <https://doi.org/10.7554/eLife.42695.019>

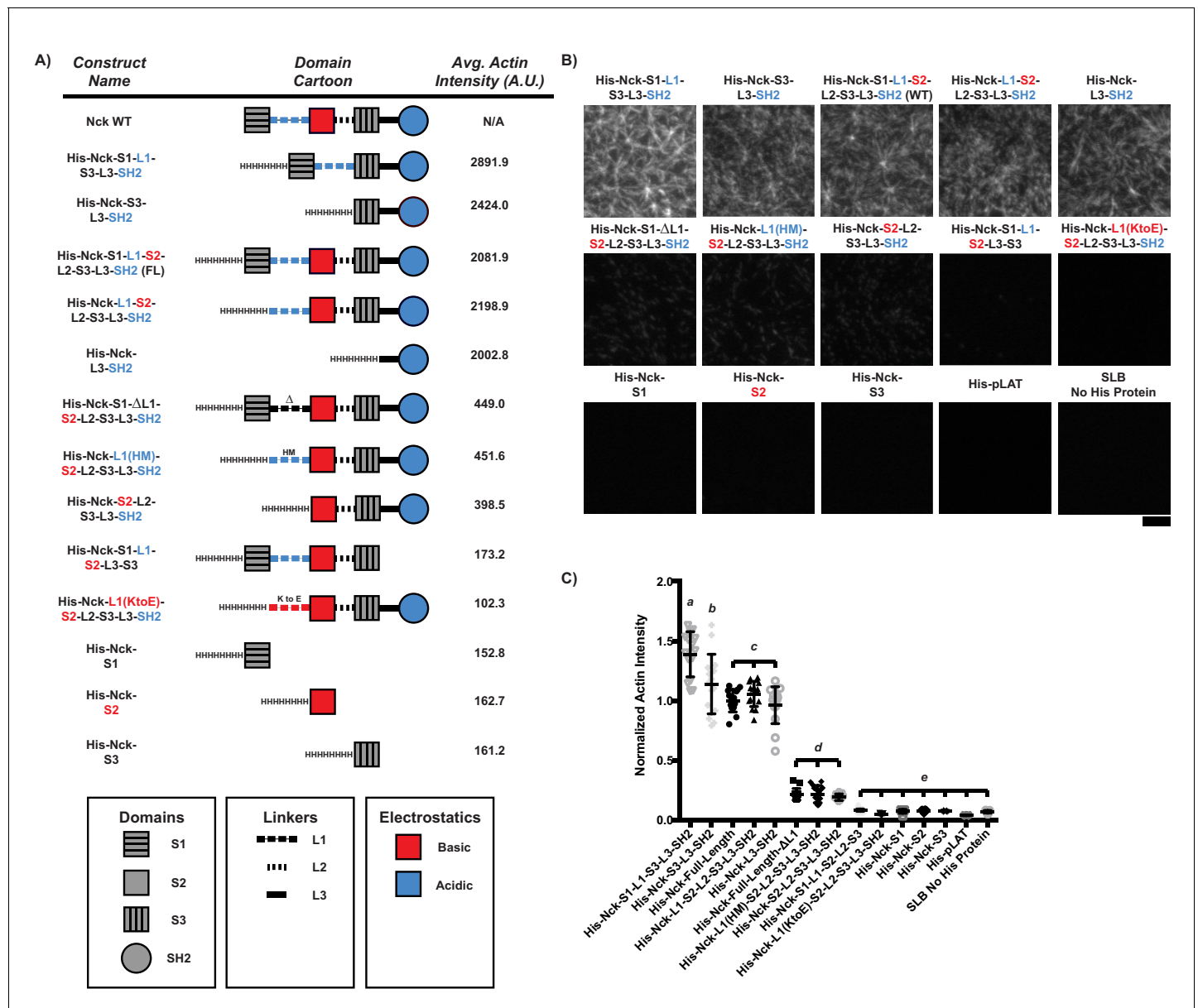


**Figure 3—figure supplement 5.** The ability of His-tagged Nck variants to recruit actin filaments to an SLB depends on the number of basic regions (concentrated in L1 and the SH2 domain) vs. the number of acidic regions (concentrated in the second SH3 domain). If the number of basic regions > the number of acidic regions, the Nck variant will recruit actin filaments. (A) Names (left), domain schematics (center), and average actin intensity recruited to the bilayer (right) for each Nck variant. (B) TIRF microscopy images of rhodamine-actin recruited to SLBs coated with His-tagged Nck variants or His-tagged pLAT as a control. Scale Bar = 5  $\mu$ m. All images set to same intensity range. (C) Normalized fluorescence intensity of rhodamine-actin (normalized to the average actin filament intensity of His-Nck-L3-SH2 experiments) recruited to SLBs coated with His-tagged Nck variants. Shown are individual data points and their mean  $\pm$  s.d. from N = 15 fields of view from three independent experiments (5 FOV per experiment). Significance was determined using analysis of variance with Tukey's multiple comparison test and found that  $p < 0.0332$  for b vs. c,  $p < 0.0021$  for d vs. e, and  $p < 0.0001$  for a vs. b, a vs. c, a vs. d, a vs. e, b vs. d, b vs. e, c vs. d, and c vs. e.

DOI: <https://doi.org/10.7554/eLife.42695.021>

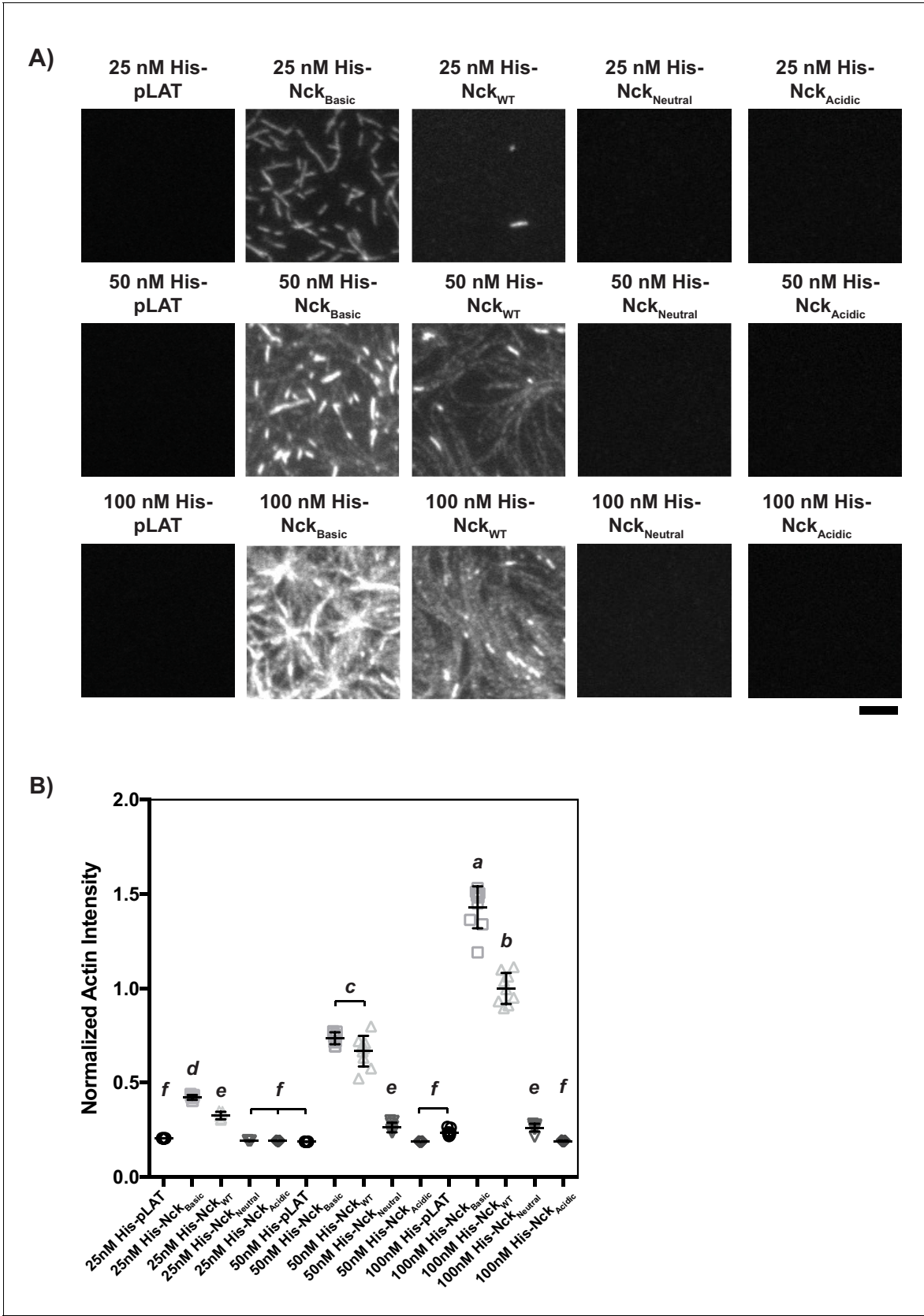


**Figure 3—figure supplement 6.** His-tagged Nck variants containing mutations to L1 recruit actin to the bilayer in a density-dependent manner when L1 is WT or contains basic mutations. (A) TIRF microscopy images of rhodamine-actin recruited to SLBs coated with His-tagged full-length Nck variants. Figure 3—figure supplement 6 continued on next page

*Figure 3—figure supplement 6 continued*

Concentrations refer to the concentration of His-tagged protein in solution used to coat the bilayer; for pLAT-Alexa488, with 2% Ni-NTA lipid and His-pLAT-Alexa488 protein in the 0–100 nM range (100 nM data is from **Figure 3B**), the density of protein recruited to the bilayer scales approximately linearly with protein concentration in solution (not shown). Scale bar = 5  $\mu$ m. All images set to same intensity range. **(B)** Normalized fluorescence intensity of rhodamine-actin (normalized to the average actin filament intensity of 100 nM His-Nck<sub>WT</sub> experiments) recruited to SLBs coated with His-tagged full-length Nck variants. Shown are individual data points and their mean  $\pm$ s.d. from N = 9 fields of view from three independent experiments (3 FOV per experiment). Significance was determined using analysis of variance with Tukey's multiple comparison test and found that  $p < 0.0332$  for e vs. f,  $p < 0.0002$  for d vs. e, and  $p < 0.0001$  for a vs. b, a vs. c, a vs. d, a vs. e, a vs. f, b vs. c, b vs. d, b vs. e, b vs. f, c vs. d, c vs. e, and c vs. f.

DOI: <https://doi.org/10.7554/eLife.42695.023>

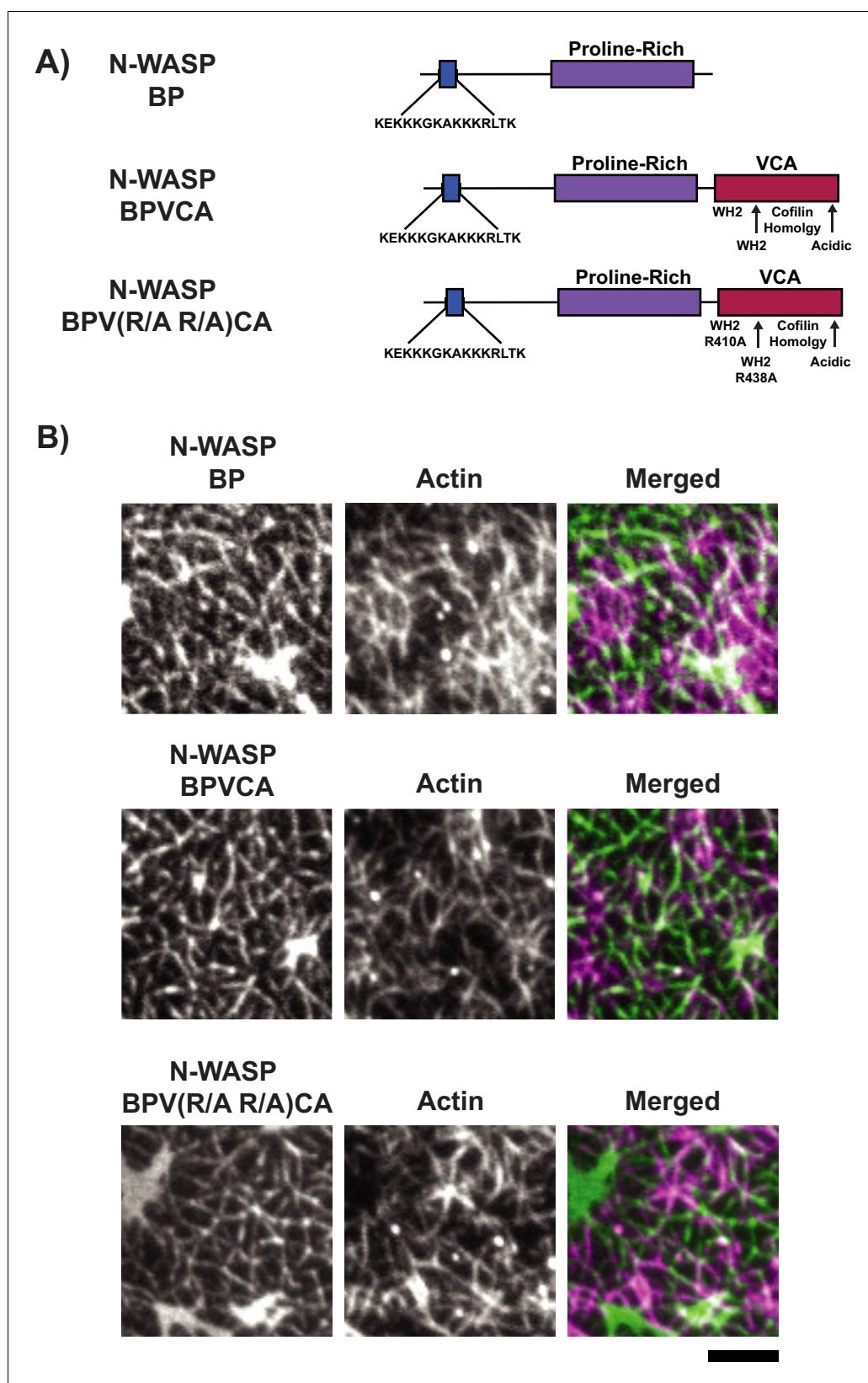


**Figure 3—figure supplement 7.** LAT condensates containing N-WASP fragments recruit actin to SLBs. (A) Schematics of N-WASP variants used to generate LAT condensates. (B) TIRF microscopy images of pLAT → N-WASP variant condensates incubated with rhodamine-labeled actin filaments. Condensates containing N-WASP

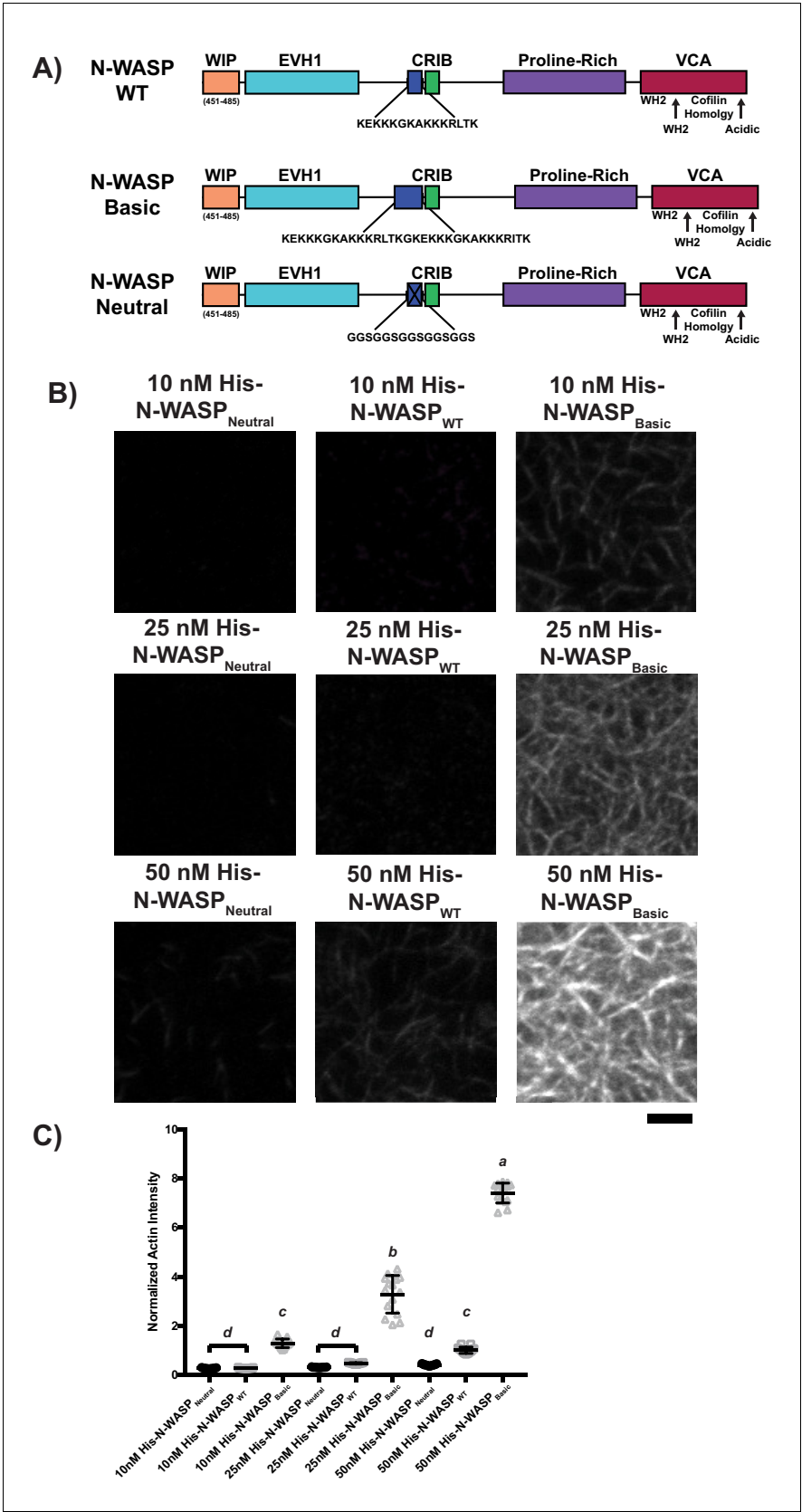
*Figure 3—figure supplement 7 continued on next page*



*Figure 3—figure supplement 7 continued*

variants strongly recruited actin filaments to SLBs. Images are representative of 3 independent experiments. Scale bar = 5  $\mu$ m. All images set to same intensity range.

DOI: <https://doi.org/10.7554/eLife.42695.025>



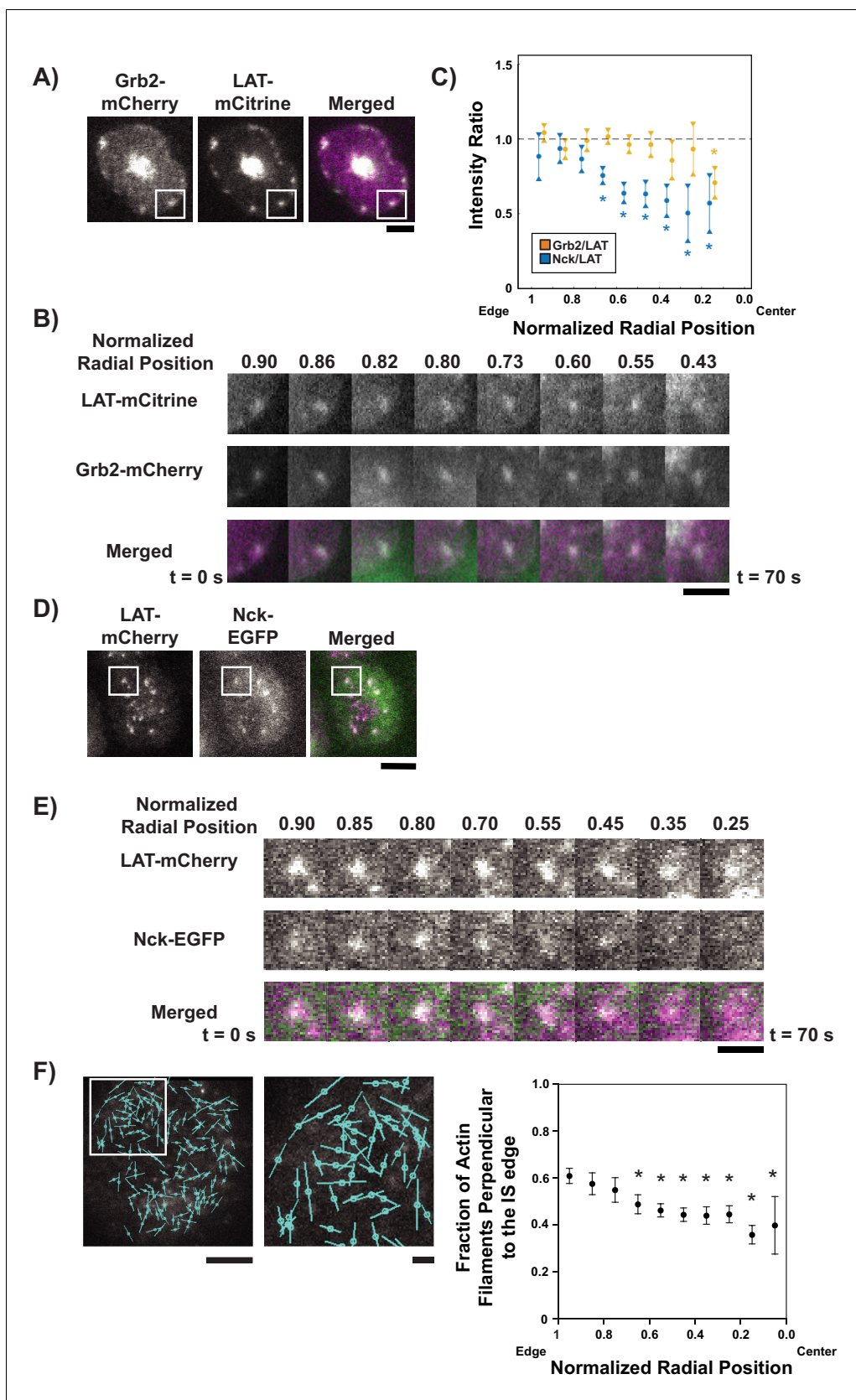
**Figure 3—figure supplement 8.** His-tagged N-WASP<sup>Neutral</sup>, N-WASP<sup>WT</sup>, or N-WASP<sup>Basic</sup> recruit actin filaments to SLBs in a density-dependent manner. (A) Schematics of full-length N-WASP variants. (B) TIRF microscopy images

Figure 3—figure supplement 8 continued on next page

*Figure 3—figure supplement 8 continued*

of rhodamine-labeled actin filaments recruited to SLBs coated with His-tagged full-length N-WASP variants. Concentrations refer to the concentration of His-tagged protein in solution used to coat the bilayer; for pLAT-Alexa488, with 2% Ni-NTA lipid and His-pLAT-Alexa488 protein in the 0–50 nM range (50 nM data is from **Figure 3C**), the density of protein recruited to the bilayer scales approximately linearly with protein concentration in solution. Scale bar = 5  $\mu\text{m}$ . All images set to same intensity range. **(C)** Normalized fluorescence intensity of rhodamine-actin (normalized to the average actin filament intensity of 50 nM His-N-WASP<sub>WT</sub> experiments) recruited to SLBs coated with His-tagged full-length N-WASP variants. Shown are individual data points and their mean  $\pm$ s.d. for N = 15 fields of view from three independent experiments (5 FOV per experiment). Significance was determined using analysis of variance with Tukey's multiple comparison test and found that  $p < 0.0001$  for a vs. b, a vs. c, a vs. d, b vs. c, b vs. d, and c vs. d.

DOI: <https://doi.org/10.7554/eLife.42695.026>

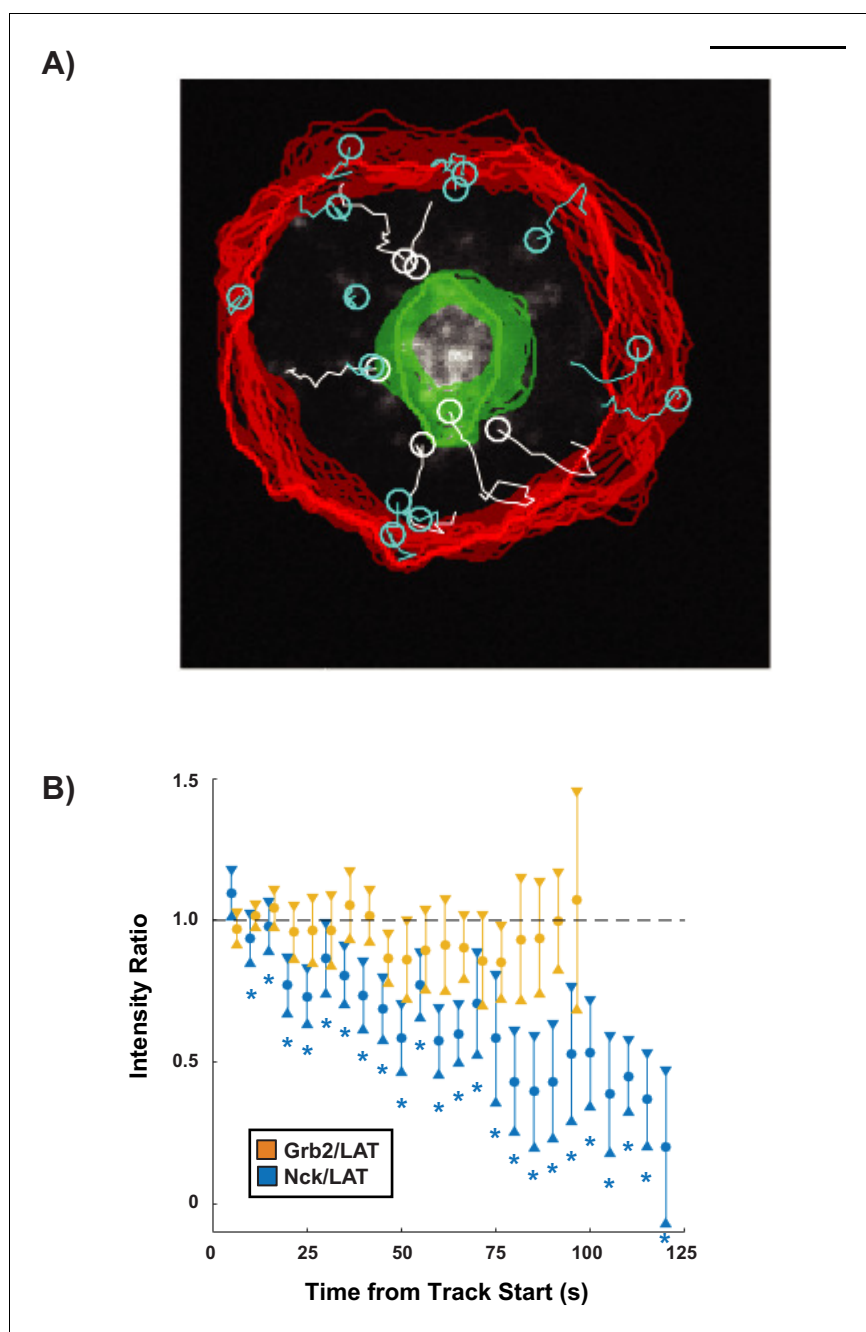


**Figure 4.** LAT condensates change composition as they move across the IS. (A) TIRF microscopy image of Jurkat T cell expressing Grb2-mCherry (magenta in merge) and LAT-mCitrine (green in merge) activated on an SLB coated with OKT3 and ICAM-1. Scale Bar = 5  $\mu\text{m}$ . (B) Magnification of Figure 4 continued on next page

## Figure 4 continued

boxed region in (A), with normalized radial position (one at synapse edge, 0 at cSMAC center) indicated above images and time indicated below. Scale bar = 2  $\mu\text{m}$ . (C) Quantification of fluorescence intensity ratios of Grb2/LAT (gold) and Nck/LAT (blue) in LAT condensates in Jurkat T cells at different normalized radial positions. Measurements were made at identical relative locations but data points are slightly offset in the graph for visual clarity. Plot displays median and its 95% confidence interval from  $N = 125$  condensates from 25 cells expressing Nck-sfGFP and LAT-mCherry from five independent experiments and 82 condensates from 11 cells expressing Grb2-mCherry and LAT-mCitrine from five independent experiments. Only tracks in which the mean Grb2 or Nck intensity was greater than one standard deviation above background during the first three measurements were used for this analysis. Asterisks indicate data points whose values differ significantly from the reference data point (radial position = 1.0–0.9 for Grb2 and radial position = 0.9–0.8 for Nck) as determined using a Wilcoxon rank-sum test with Bonferroni correction. The Bonferroni correction was used to achieve a total type-I error of 0.05. For eight comparisons, this leads to a significance threshold per pair = 0.006. (D) TIRF microscopy image of Jurkat T cell expressing Nck-sfGFP (green in merge) and LAT-mCherry (magenta in merge) activated on an SLB by OKT3 and ICAM-1. Scale Bar = 5  $\mu\text{m}$ . (E) Magnification of boxed region in (D). Scale bars and details as in (B). (F) Fluorescence polarization microscopy image of a Jurkat T cell sparsely labeled with SiR-Actin and activated on an SLB coated with OKT3 and ICAM-1 (left, scale bar = 10  $\mu\text{m}$ ), magnification of boxed region in image (middle, scale bar = 2  $\mu\text{m}$ ), and fraction of filaments perpendicular ( $+/-45^\circ$ ) to the synapse edge (right). Cyan lines in left and center images indicate the orientation of the fluorescence dipole of the SiR fluorophore which in turn is oriented orthogonal to the underlying actin filament (see **Figure 4—figure supplement 5**). Shown are the mean  $\pm$ s.d. from  $N = 13,052$  particles from 6 cells. Asterisks indicate data points whose values differ significantly from the reference data point (radial position = 1.0–0.9) as determined using a t-test with Bonferroni correction to achieve a total type-I error of 0.05.

DOI: <https://doi.org/10.7554/eLife.42695.033>



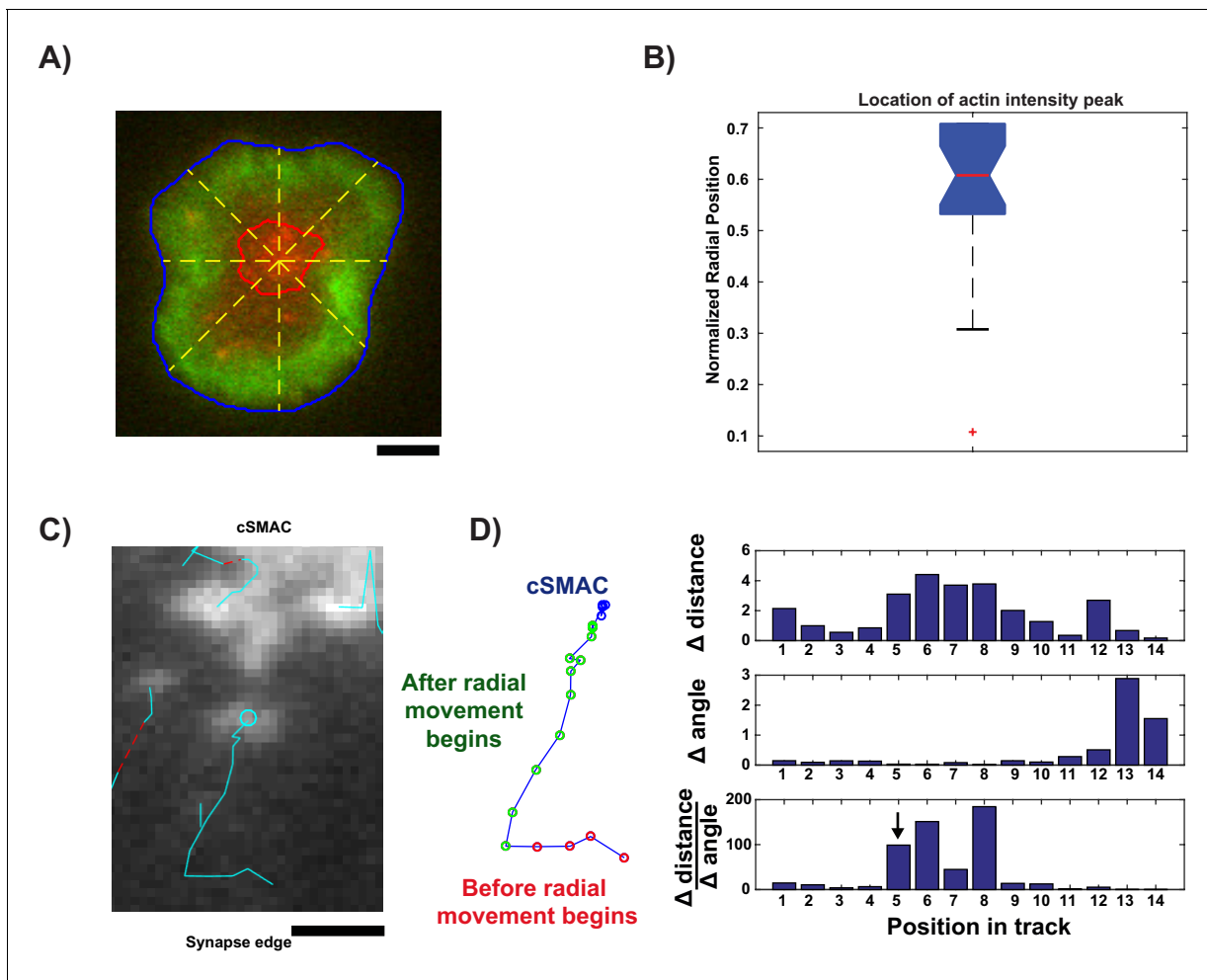
**Figure 4—figure supplement 1.** Nck dissipation from condensates is spatially regulated within the first 5 min of synapse formation. (A) Example of analysis overlaid on a cell showing tracks of individual LAT condensates that move radially over the course of the time-lapse (white), LAT condensates tracks that do not move radially over the course of the time-lapse (cyan), the synapse edge over the course of the time-lapse (red), and the cSMAC over the course of the time-lapse (green). For information regarding detection of the synapse edge and cSMAC, see section 4A of the Supplemental Methods. Tracks that did not move radially (cyan) were discarded from the analysis. (B) Nck/LAT (blue) and Grb2/LAT (orange) ratios in condensates plotted against time. The ratio of Grb2: LAT remains constant over time while the ratio of Nck: LAT steadily decreases over time. Plot displays median and its 95% confidence interval from  $N = 125$  condensates from 25 cells expressing Nck-sfGFP and LAT-mCherry from five independent experiments and 82 condensates from 11 cells expressing Grb2-mCherry and LAT-mCitrine from five independent experiments (same condensate trajectories used in **Figure 4C**, just aligned differently). Asterisks indicate data points whose values differ significantly from the reference data point (time = 0 s) as determined

Figure 4—figure supplement 1 continued on next page

*Figure 4—figure supplement 1 continued*

using a Wilcoxon rank-sum test with Bonferroni correction. The Bonferroni correction was used to achieve a total type-I error of 0.05. For 23 comparisons, this leads to a significance threshold per pair = 0.002.

DOI: <https://doi.org/10.7554/eLife.42695.034>



**Figure 4—figure supplement 2.** Image analysis for live cell data. (A) Example cell (LAT channel: red, LifeAct (actin) channel: green) overlaid with segmented synapse edge (blue line), segmented cSMAC edge (red line), and lines from cSMAC center to synapse edge (yellow dashed lines, 45° angles between neighboring lines) to measure actin intensity radial profile. (B) Box plot of the normalized radial position at which the actin intensity profile along each line (yellow dashed lines in (A)) reaches its maximum, for each time point in each cell. Box plot description: red central mark shows median; box edges show 25th and 75th percentiles; dashed whiskers extend to the most extreme data points not designated as 'outliers'; and notch emanating from median indicates the 95% confidence interval around the median, shown for visual aid. (C) Example of condensate that is tracked before and after radial movement. (D) (left) Example track from C, segmented into three distinct regions: before actin engagement (red), after actin engagement (green), and inside cSMAC (blue). (right) Measurements used to detect when condensates begin to move radially: frame-to-frame change in distance to cSMAC center (top), frame-to-frame change in angle between consecutive displacements (middle), and ratio of previous two measurements (bottom). Arrow indicates position chosen based on the first ratio value in the top 10<sup>th</sup> percentile.

DOI: <https://doi.org/10.7554/eLife.42695.035>



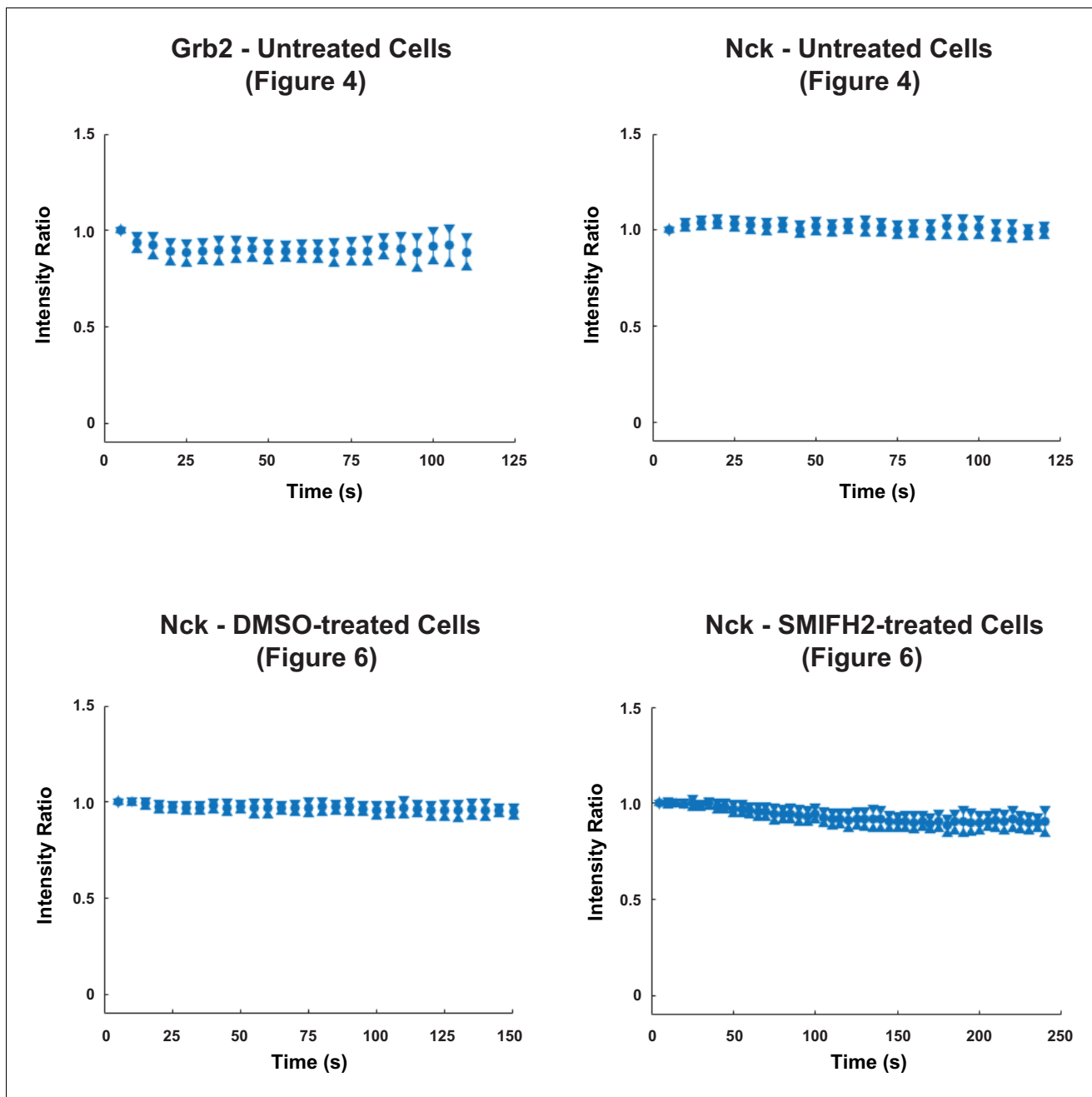


**Figure 4—figure supplement 3.** Photobleaching analysis of live-cell data. The mean intensity within the segmented synapse, but outside the segmented cSMAC and detected condensate areas, was taken for each cell for every frame. All mean intensity measurements were normalized by the mean intensity of the first frame for each cell. The ratio of pooled normalized mean intensity (either Grb2: LAT or Nck: LAT) was plotted as a minimal boxplot showing only the median and notches, indicating the 95% confidence interval of each median. This analysis demonstrates that the two channels in live-cell time lapses exhibited similar photobleaching rates (which were overall minimal), and thus variable photobleaching did not contribute to the observed condensate composition changes over time.

DOI: <https://doi.org/10.7554/eLife.42695.036>

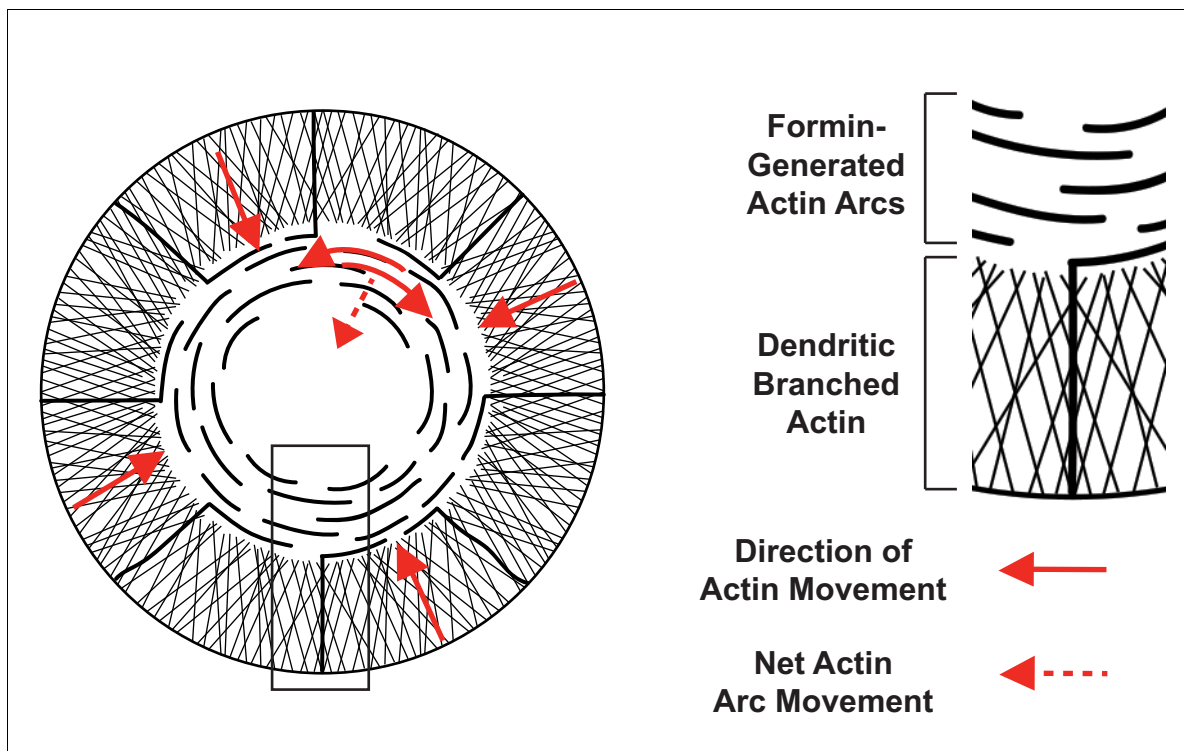


**Figure 4—figure supplement 4.** Two actin networks at the IS, with different architecture and movement. (Left) Schematic of actin filament networks and direction of movement at the IS. In the outer region, a dendritic branched actin network undergoes retrograde flow approximately perpendicular to the edge of the synapse (solid red arrows at synapse edge). In the medial region, contractile actin arcs sweep towards the center of the synapse. Actin arcs move parallel to the synapse edge (solid red arrows; filaments sliding against each other through the action of myosin II). Parallel movement results in net movement that is perpendicular to the edge via a telescoping mechanism in which filament motion ‘closes’ the circular architecture (dotted red arrow; much like the diaphragm of a camera). (Right) Enlarged view of boxed region from schematic on left with dendritic branched actin network and formin-generated actin arcs.

DOI: <https://doi.org/10.7554/eLife.42695.037>

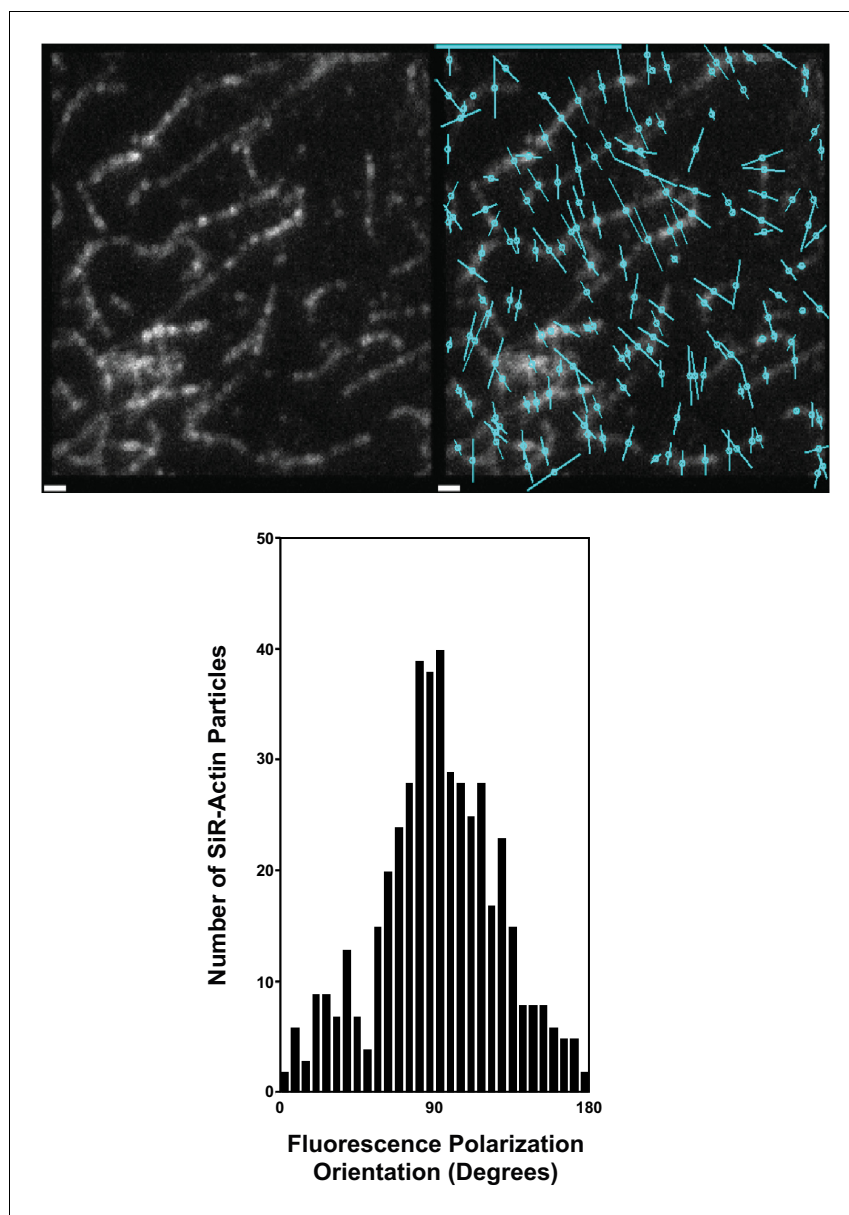


**Figure 4—figure supplement 5.** SiR-Actin polarity is perpendicular to actin filaments. (top, left) SiR-Actin labeling of immobilized actin filaments attached to a glass coverslip. (top, right) The polarity of SiR-Actin bound to immobilized actin filaments is shown by circles transversed by a line to indicate the dye polarity (cyan). (bottom) Histogram showing the orientation of SiR-Actin bound to actin filaments with respect to the alignment of the actin filament. Scale Bar = 1  $\mu$ m.

DOI: <https://doi.org/10.7554/eLife.42695.038>

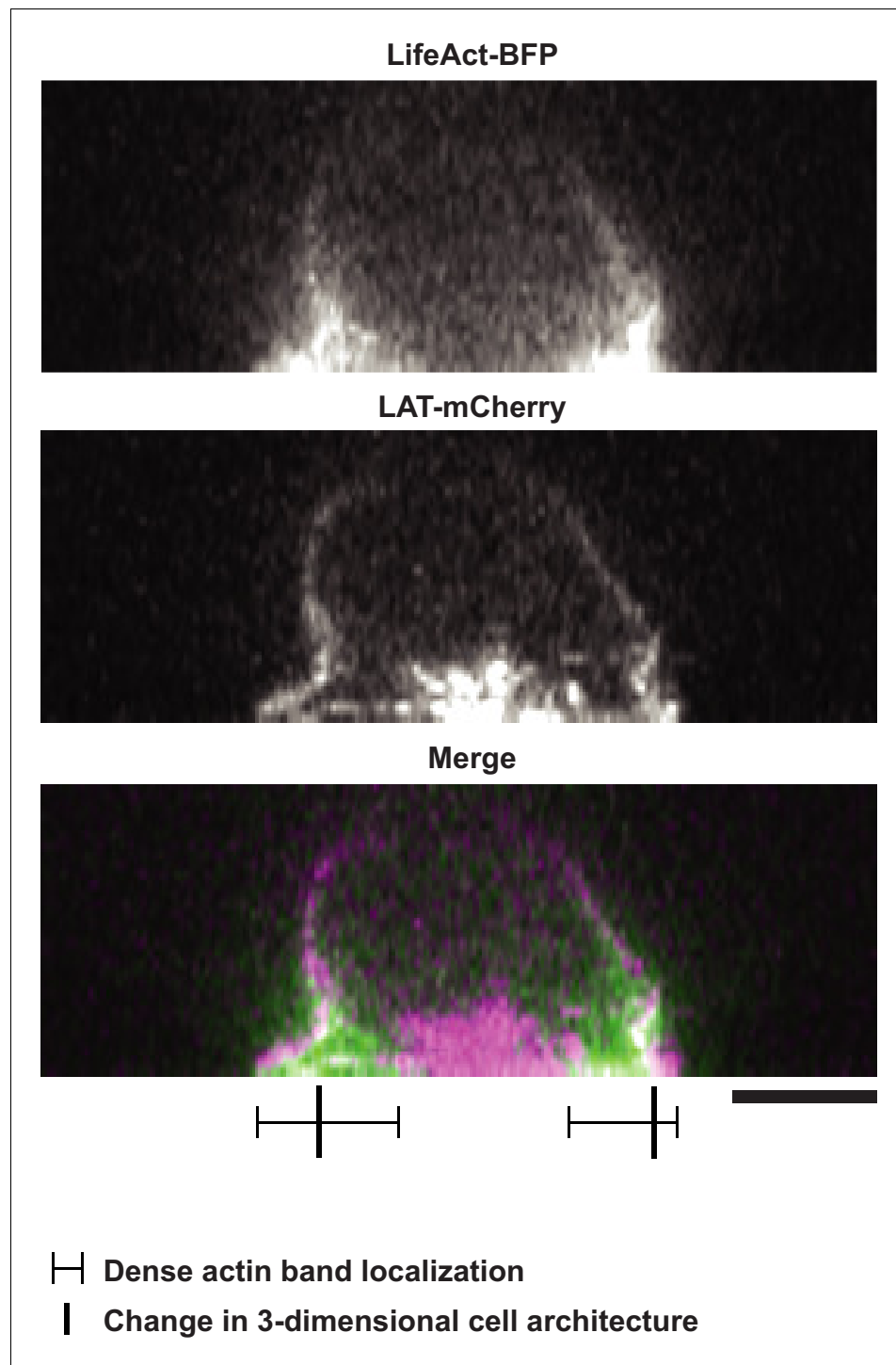


**Figure 4—figure supplement 6.** The two-dimensional extension of the dense actin network at the IS in Jurkat T cells activated on SLBs is independent of the three dimensional shape of the activated Jurkat T cell. Scale Bar = 5  $\mu$ m.

DOI: <https://doi.org/10.7554/eLife.42695.039>

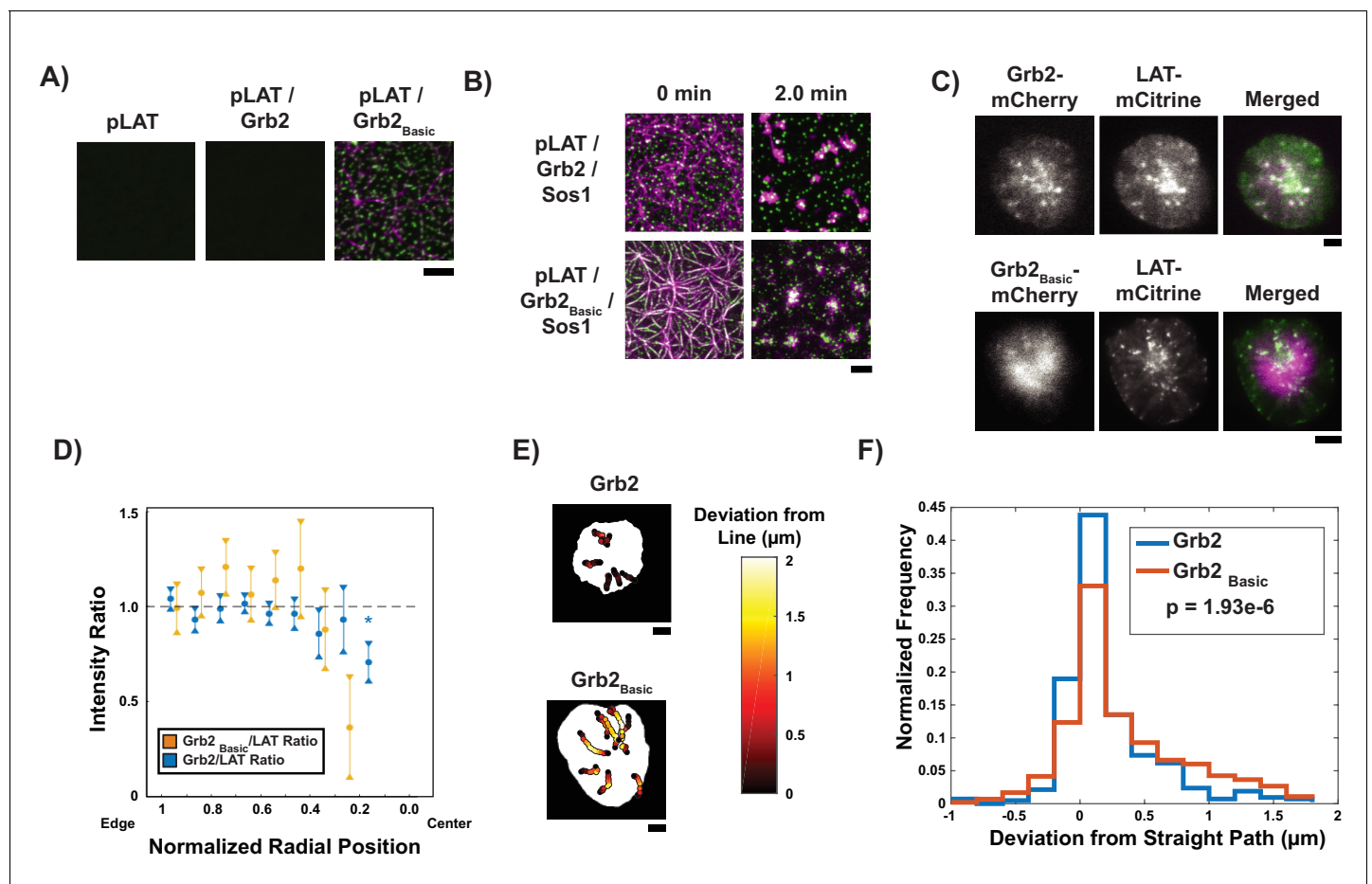


**Figure 5.** Grb2 fused to a basic molecular clutch can couple LAT condensates to actin. (A) TIRF microscopy images of rhodamine-actin recruited to SLBs by His-tagged pLAT or condensates of pLAT → Grb2 or pLAT → Grb2<sub>Basic</sub>. Scale bar = 5 μm. (B) TIRF microscopy images of pLAT → Sos1 condensates containing Grb2<sub>WT</sub> (top row; data from **Figure 2**) or Grb2<sub>Basic</sub> (bottom row) formed in an actin network before (t = 0 min) and after (t = 2 min) addition of myosin II. Actin shown in magenta and LAT condensates in green. Scale bar = 5 μm. (C) TIRF microscopy image of Jurkat T cell expressing Grb2-mCherry (top, magenta in merge) or Grb2<sub>Basic</sub>-mCherry (bottom, magenta in merge) and LAT-mCitrine (green in merge) activated on an SLB coated with OKT3 and ICAM-1. Scale Bar = 5 μm. (D) Fluorescence intensity ratios of Grb2/LAT (blue, data from **Figure 4C**) or Grb2<sub>Basic</sub> / LAT (gold) in condensates at different normalized radial positions. Measurements were made at identical relative locations but data are slightly offset in the graph for visual clarity. Plot displays median and notches from boxplot for 95% confidence interval from N = 44 condensates from 12 cells expressing Grb2<sub>Basic</sub>-mCherry and LAT-mCitrine from seven independent experiments and 82 condensates from 11 cells expressing Grb2-mCherry and LAT-mCitrine from five independent experiments (same cells as in **Figure 4C**). Only tracks in which the mean Grb2 or Grb2<sub>Basic</sub> intensity was greater than one standard deviation above background during the first three measurements were used to generate this plot. Asterisk indicates data point whose value differs significantly from the reference data point (radial position = 1.0–0.9) as determined using a Wilcoxon rank-sum test with Bonferroni correction. The Bonferroni correction was used to achieve a total type-I error of 0.05. For eight comparisons, this leads to a significance threshold per pair = 0.006. (E) Trajectories of LAT condensates in Jurkat T cells expressing Grb2-mCherry (top) or Grb2<sub>Basic</sub>-mCherry (bottom) recorded over 2 to 5 min of imaging. Trajectories are color-coded as indicated in the legend at right according to deviation from a straight line between the estimated starting point of actin engagement and just before entering the cSMAC (see Materials and methods). Scale bar = 5 μm. (F) Distribution of deviations from a straight line for condensates in Jurkat T cells expressing Grb2-mCherry (red) or Grb2<sub>Basic</sub>-mCherry (blue). N = 44 condensates from 12 cells expressing Grb2<sub>Basic</sub>-mCherry and LAT-mCitrine from seven independent experiments and 82 condensates from 11 cells expressing Grb2-mCherry and LAT-mCitrine from independent experiments (same cells as in **Figure 4C**). P-value is for comparing the two distributions via a Kolmogorov-Smirnov test. Only tracks in which the mean Grb2 or Grb2<sub>Basic</sub> intensity was greater than one standard deviation above background during the first three measurements were used to generate this plot.

DOI: <https://doi.org/10.7554/eLife.42695.043>

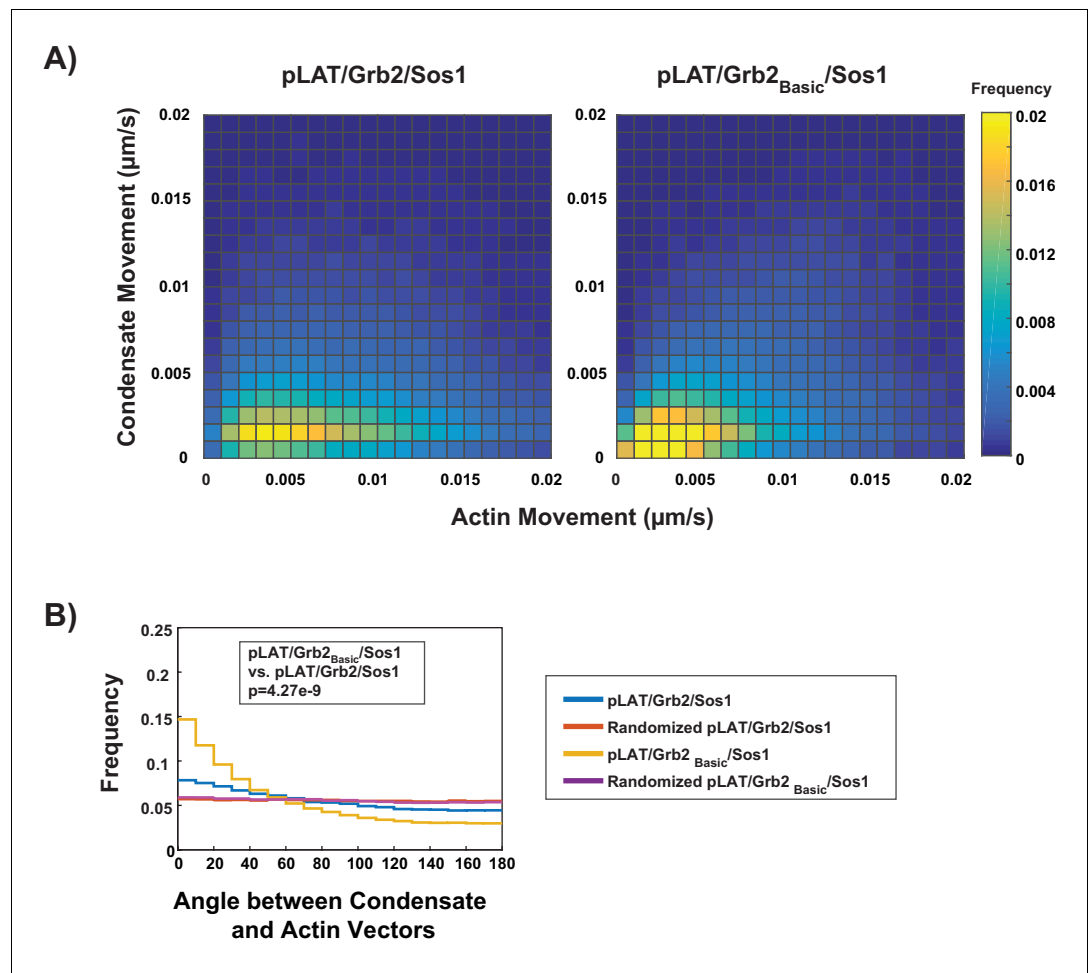


**Figure 5—figure supplement 1.** Adding a doubled N-WASP basic domain to Grb2 (Grb2<sub>Basic</sub>) enables pLAT / Grb2<sub>Basic</sub>/Sos1 condensates to move with actin to a better degree than condensates formed with WT Grb2. (A) Condensate speed vs. actin speed for pLAT/Grb2/Sos1 (from **Figure 3**) or pLAT / Grb2<sub>Basic</sub>/Sos1 condensates in contracting actin networks from STICS analysis. Type of condensate indicated above each heat map. Heat map indicates frequency in each bin, that is counts in each bin normalized by total number of counts. (B) Distribution of the angle between actin and condensate movement vectors for pLAT/Grb2/Sos1 (blue, from **Figure 3**), pLAT / Grb2<sub>Basic</sub>/Sos1 (gold), randomized pLAT/Grb2/Sos1 (red, from **Figure 3**), or randomized pLAT / Grb2<sub>Basic</sub>/Sos1 (purple). Data in (A) and (B) were pooled from N = 15 fields of view from three independent experiments (5 FOV per experiment).

DOI: <https://doi.org/10.7554/eLife.42695.044>

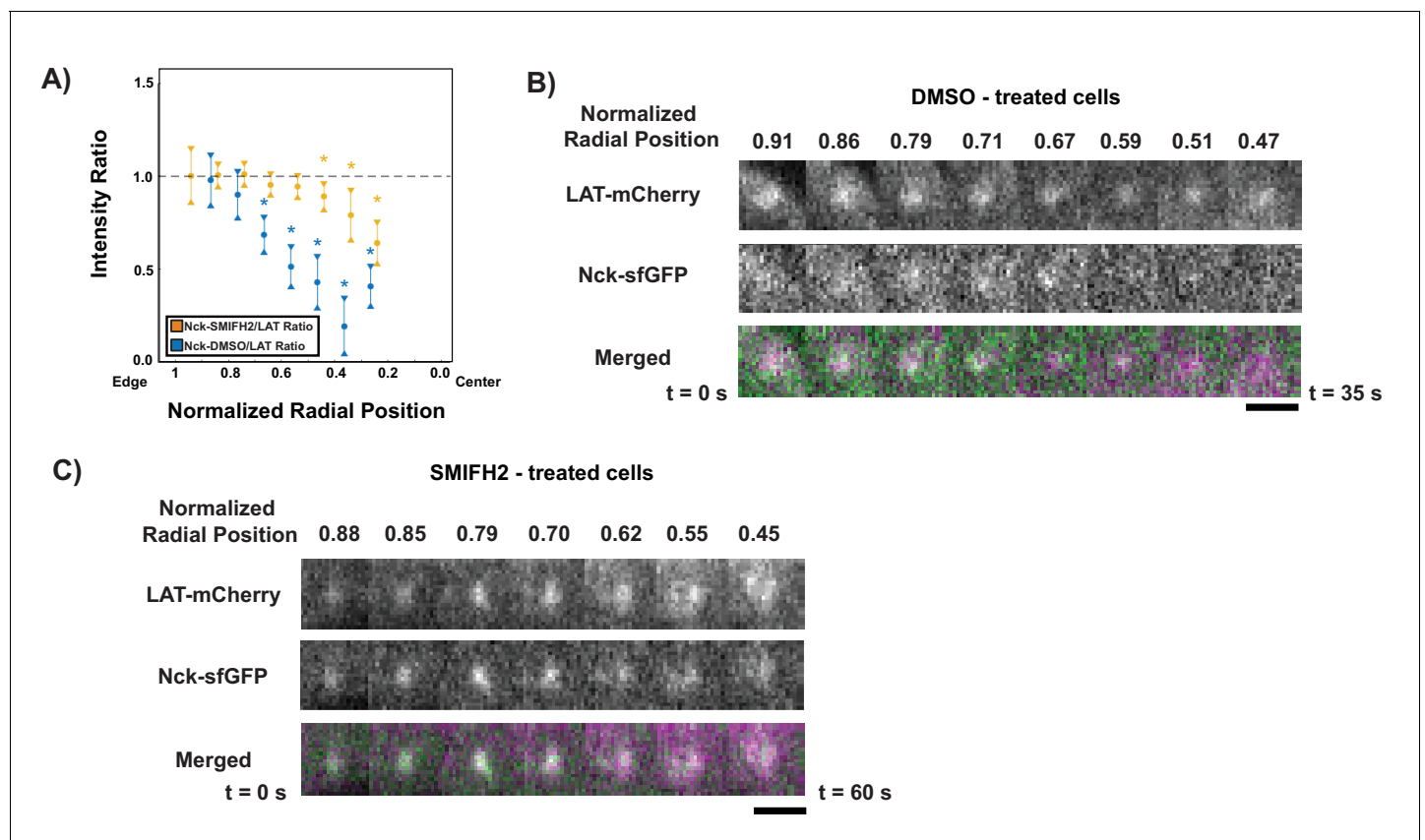


**Figure 6.** Formin activity is necessary for Nck dissipation from LAT condensates. (A) Fluorescence intensity ratios of Nck/LAT in condensates in Jurkat T cells treated with DMSO (blue) or the formin inhibitor, SMIFH2, (gold) at different normalized radial positions. Measurements were made at identical relative locations but data are slightly offset in the graph for visual clarity. Plot displays median and notches from boxplot for 95% confidence interval from N = 43 condensates from 11 DMSO-treated cells from five individual experiments and 102 condensates from 14 SMIFH2-treated cells from five individual experiments. Only tracks in which the mean Nck intensity was greater than one standard deviation above background during the first three measurements were used to generate this plot. The first DMSO data point (radial position = 1.0–0.9) does not appear in the plot because the number of detected condensates was too small (<10) to generate a statistically meaningful measurement. Asterisks indicate data points whose values differ significantly from the reference data point (radial position = 0.9–0.8) as determined using a Wilcoxon rank-sum test with Bonferroni correction. The Bonferroni correction was used to achieve a total type-I error of 0.05. For eight comparisons, this leads to a significance threshold per pair = 0.006. (B, C) Magnification of boxed regions from **Figure 6—figure supplement 1** of condensates containing LAT-mCherry (magenta in merge) and Nck-sfGFP (green in merge) during their trajectories across the IS in a cell treated with DMSO (B) or SMIFH2 (C). Normalized radial position indicated above image panels and time below panels. Scale bar = 2  $\mu$ m.

DOI: <https://doi.org/10.7554/eLife.42695.047>



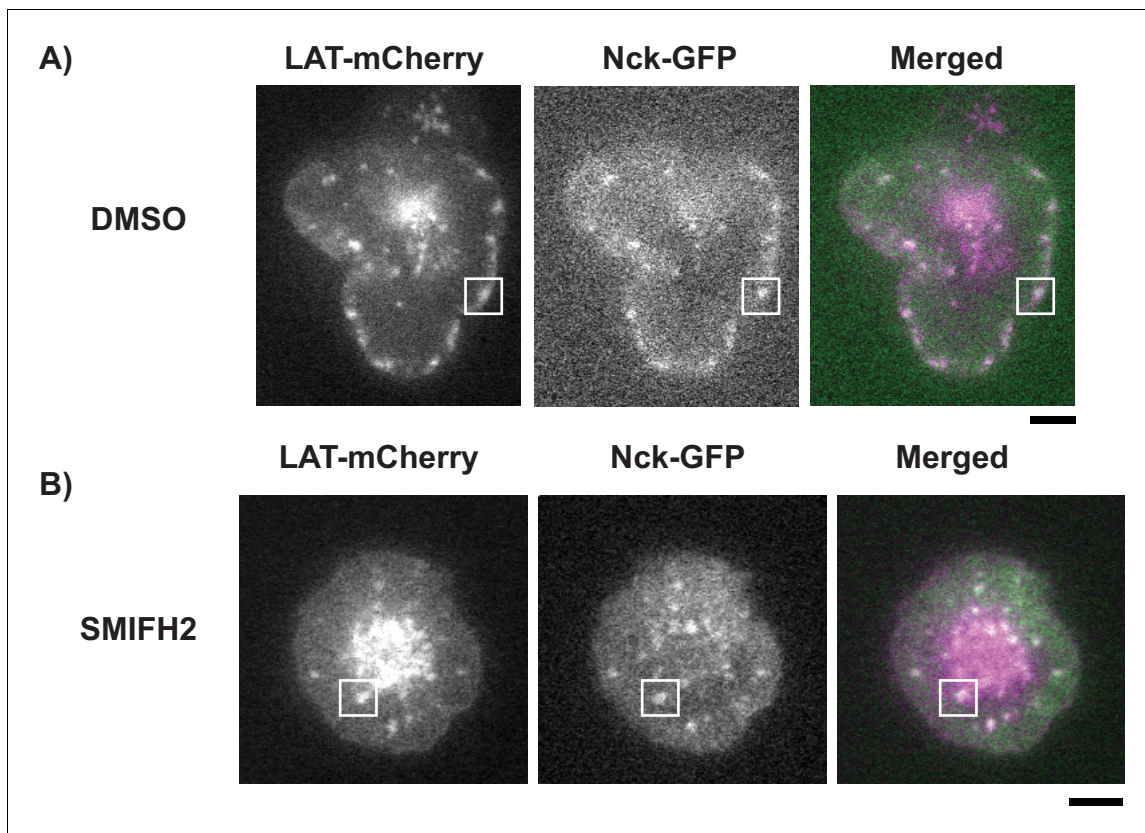


**Figure 6—figure supplement 1.** Example images showing DMSO- or SMIFH2-treated Jurkat T cells activated on SLBs. (A, B) TIRF microscopy images of Jurkat T cells expressing Nck-sfGFP and LAT-mCherry and treated with DMSO (A) or the formin inhibitor SMIFH2 (B) for 5 min prior to activation on SLBs. Scale Bars = 5  $\mu$ m.

DOI: <https://doi.org/10.7554/eLife.42695.048>